Inorganic Chemistry

Article

pubs.acs.org/IC

Long-Lived Room Temperature Deep-Red/Near-IR Emissive Intraligand Triplet Excited State (^{3}IL) of Naphthalimide in Cyclometalated Platinum(II) Complexes and Its Application in Upconversion

Wenting Wu, Huimin Guo, Wanhua Wu, Shaomin Ji, and Jianzhang Zhao*

State Key Laboratory of Fine Chemicals, School of Chemical Engineering, Dalian University of Technology, E-208 West Campus, 2 Ling Gong Road, Dalian 116024, China

Supporting Information

ABSTRACT: [C^NPt(acac)] (C^N = cyclometalating ligand; acac = acetylacetonato) complexes in which the naphthalimide (NI) moiety is directly cyclometalated (NI as the C donor of the C−Pt bond) were synthesized. With 4-pyrazolylnaphthalimide, isomers with five-membered (**Pt-2**) and six-membered (**Pt-3**) chelate rings were obtained. With 4-pyridinylnaphthalimide, only the complex with a five-membered chelate ring (**Pt-4**) was isolated. A model complex with 1-phenylpyrazole as the C^N ligand was prepared (**Pt-1**). Strong absorption of visible light (ε = 21 900 M^{-1} cm^{-1} at 443 nm for **Pt-3**) and room temperature (RT) phosphorescence at 630 nm (**Pt-2** and **Pt-3**) or 674 nm (**Pt-4**) were observed. Long-lived phosphorescences were observed for **Pt-2** (τ_P = 12.8 μs) and **Pt-3** (τ_P = 61.9 μs). **Pt-1** is nonphosphorescent at RT in solution because of the acac-localized T_1 excited state [based on density functional theory (DFT) calculations and spin density analysis], but a structured emission band centered at 415 nm was observed at 77 K. Time-resolved transient absorption spectra and spin density analysis indicated a NI-localized intraligand triplet excited state (^{3}IL) for complexes **Pt-2**, **Pt-3**, and **Pt-4**. DFT calculations on the transient absorption spectra ($T_1 \rightarrow T_n$ transitions, $n > 1$) also support the ^{3}IL assignment of the T_1 excited states of **Pt-2**, **Pt-3**, and **Pt-4**. The complexes were used as triplet sensitizers for triplet−triplet-annihilation (TTA) based upconversion, and the results show that **Pt-3** is an efficient sensitizer with an upconversion quantum yield of up to 14.1%, despite its low phosphorescence quantum yield of 5.2%. Thus, we propose that the sensitizer molecules at the triplet excited state that are otherwise nonphosphorescent were involved in the TTA upconversion process, indicating that weakly phosphorescent or nonphosphorescent transition-metal complexes can be used as triplet sensitizers for TTA upconversion.

1. INTRODUCTION

Luminescent platinum(II) complexes have attracted much attention because of applications in electroluminescence, photocatalysis, molecular probes, etc.[1−12] The light-harvesting and properties of triplet excited states of these complexes are crucial for new applications, such as photocatalysis[13−15] or phosphorescent molecular probes.[11,15−19] We demonstrated that O_2 sensing properties can be improved with long-lived ^{3}IL (triplet intraligand) excited states, compared to that with normal ^{3}MLCT (triplet metal-to-ligand charge-transfer) excited states.[18,19] Recently, we found that the long-lived ^{3}IL excited state of the ruthenium(II) polyimine complex can improve the efficiency of triplet−triplet-annihilation (TTA) upconversion by 10-fold, compared to the ruthenium(II) complexes with normal ^{3}MLCT excited states.[10]

Previously, we prepared pyrene-containing cyclometalated platinum(II) complexes (**Pt-6**, **Pt-7**, and **Pt-8**; Scheme 1).[6,7] We also prepared a platinum(II) bis(acetylide) complex in which the 1,8-naphthalimide (NI) is attached to a Pt^{II} ion via an acetylide bond (−C≡C−)(**Pt-11**); room temperature (RT) phosphorescence (λ_{em} = 621 nm) of the NI moiety was observed (in solution).[19,20] More recently, we linked the NI moiety to the 2-phenylpyridine (ppy) ligand and found that the lifetime (τ) of the resulting cyclometalated platinum(II) complex was prolonged to 25.5 μs, versus 2.6 μs for model complex [ppyPt(acac)] (**Pt-9** and **Pt-10**, where acac = acetylacetonato; Scheme 1).[8] However, we noticed the limitations of the current development of cyclometalated platinum(II) complexes: (1) UV−vis absorption is usually limited to the UV region;[1,21−23] (2) phosphorescence lifetimes, or more generally, the T_1 triplet excited-state lifetimes, are usually less than 5.0 μs. Transition-metal complexes with visible-light-absorbing and long-lived triplet excited states are desired for applications in, for instance, photocatalysis and photovoltaics.[12] On the basis of our previous results and the elegant works of Thompson et al.,[24,25] we propose that the direct cyclometalation of an organic chromophore (C donor of the C−metal bond) is a powerful approach to access the transition-metal complexes, for example, the cyclometalated

Received: June 11, 2011
Published: October 26, 2011

Scheme 1. Selected Cyclometalated Platinum(II) Complexes and [N^N Platinum Bis(acetylide)] Complexes with Pyrene or NI Subunits That Show Prolonged Phosphorescent Lifetimes (τ)

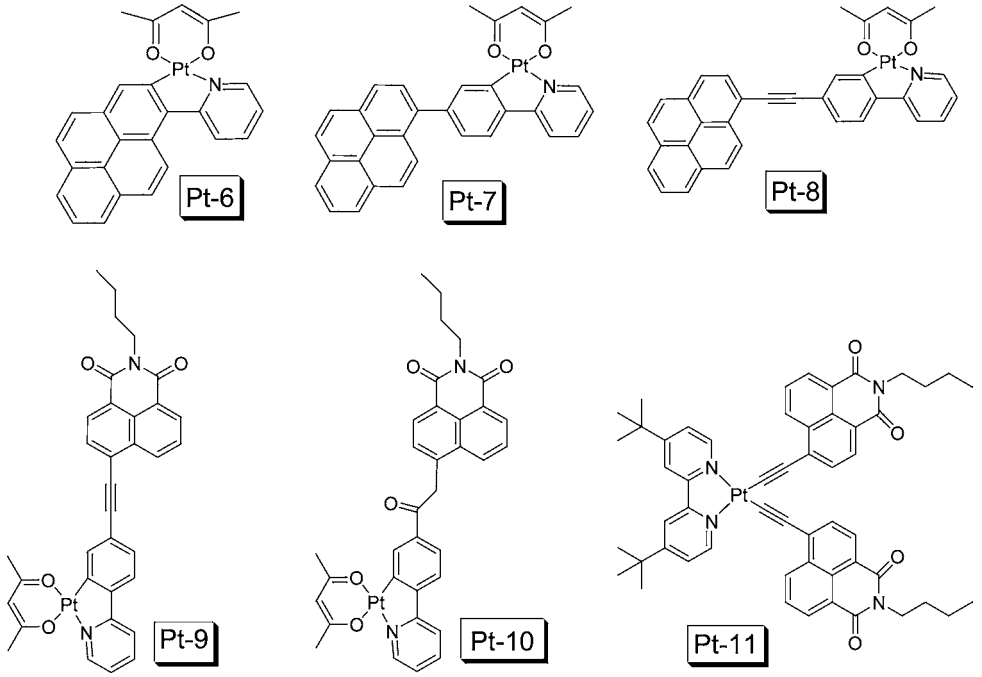

platinum(II) complexes, that show strong absorption in the visible range and, at the same time, the long-lived triplet excited states.

Concerning this aspect, NI is a versatile chromophore and has been extensively used in fluorescent molecular probes.[26,27] However, application of the NI moiety in phosphorescence is rare.[8,20,28,29] To the best of our knowledge, the RT phosphorescence of NI (in solution) was not reported until very recently in one case with platinum(II) bis(acetylide) complexes (**Pt-11**; Scheme 1).[19,20] Thus, much room is left for exploration of the role of the NI moiety in modulation of the photophysics of cyclometalated platinum(II) complexes.

In order to tackle the aforementioned limitations, herein we prepared cyclometalated platinum(II) complexes with the NI subunits *directly cyclometalated* (NI as the C donor of the C−Pt bond; **Pt-2**, **Pt-3**, and **Pt-4**). **Pt-1** was prepared as the model complex (Scheme 2). Pyrazole or pyridine was selected as the N donor of the C^N ligand. Coordination isomers with five- and six-membered rings were obtained. The complexes show strong absorption in the visible region, RT deep-red/near-IR emission (λ_{em} is up to 674 nm), and long-lived ^{3}IL excited states (the triplet excited-state lifetime is up to 61.9 μs). Furthermore, coordination isomers **Pt-2** and **Pt-3** show drastically different absorption and emission features. The complexes were used as triplet sensitizers for TTA-based upconversion, and a remarkable upconversion quantum yield (Φ_{UC}) of 14.1% was observed, with an anti-Stokes shift of 0.48 eV.

2. RESULTS AND DISCUSSION

2.1. Synthesis of the Ligands and Cyclometalated Platinum(II) Complexes. Previously, we prepared NI-containing cyclometalated platinum(II) complexes with a −C≡C− or −CH_2− linker between NI and the ppy coordination center (**Pt-9** and **Pt-10**; Scheme 1).[8] The red-shifted emission wavelength (638 nm) and prolonged phosphorescence lifetime (τ_P = 25.5 μs) were observed compared to [ppyPt(acac)] (λ_{em} = 486 nm; τ = 2.6 μs). However, UV−vis absorption of **Pt-9** and **Pt-10** is centered at ca. 400 nm.

We envisaged that the direct cyclometalation of a chromophore, for example, with NI as the C donor for the C−Pt bonds, will substantially perturb the electronic structure of the NI fluorophore, and thus UV−vis absorption may be greatly red-shifted.[24] Along these lines, herein we devised a new NI-containing ligand to prepare platinum(II) complexes with the NI moiety *directly cyclometalated*; i.e., the C atoms of the C−Pt bond is from the 3- and 5-C of the NI moiety (**Pt-2**, **Pt-3**, **Pt-4**, and **Pt-5**; Scheme 2). We anticipated that, for these complexes, the triplet excited state with a significant ^{3}IL component can be populated with photoexcitation; thus, a long emission wavelength and a prolonged phosphorescence lifetime may be observed.

Pyrazole or pyridine was selected as the N donor and NI was used as the C donor to assemble the C^N cyclometalation ligand (Scheme 2), which was prepared via the Suzuki cross-coupling reaction or nucleophilic substitution of 4-bromo-1,8-naphthalimide with pyrazole. For both types of C^N ligands, 4-bromo-*N*-butyl-1,8-naphthalimide was used as the starting material. Refluxing of *N*-butyl-4-bromo-1,8-naphthalimide with pyrazole gives the ligand **L-2** in satisfying yield. For preparation of the NI/pyridine ligand **L-3**, palladium-catalyzed Suzuki coupling was used. We propose that the different binding angles and electronic properties of the pyrazole- or pyridine/NI ligand may affect the photophysical properties of the cyclometalated complexes.[1,21,23]

The cyclometalated platinum(II) complexes were prepared by routine methods. Interestingly, for ligand **L-2**, the Pt−C bonds are formed at either the 3 or 5 position of the NI moiety; as a result, complexes **Pt-2** and **Pt-3** were obtained, respectively. The structures were assigned by ^{1}H NMR spectroscopy (see the Supporting Information). For the pyridine-containing ligand **L-3**, however, only one isomer

dx.doi.org/10.1021/ic201254w | *Inorg. Chem.* 2011, 50, 11446–11460

Scheme 2. Synthesis of the 4-Pyrazolyl- and 4-Pyridinylnaphthalimide C^N Ligands (L-2 and L-3) and the Cyclometalated Platinum(II) Complexes Pt-1, Pt-2, Pt-3, Pt-4, [ppyPt(dpm)], and [ppyPt(acac)][a]

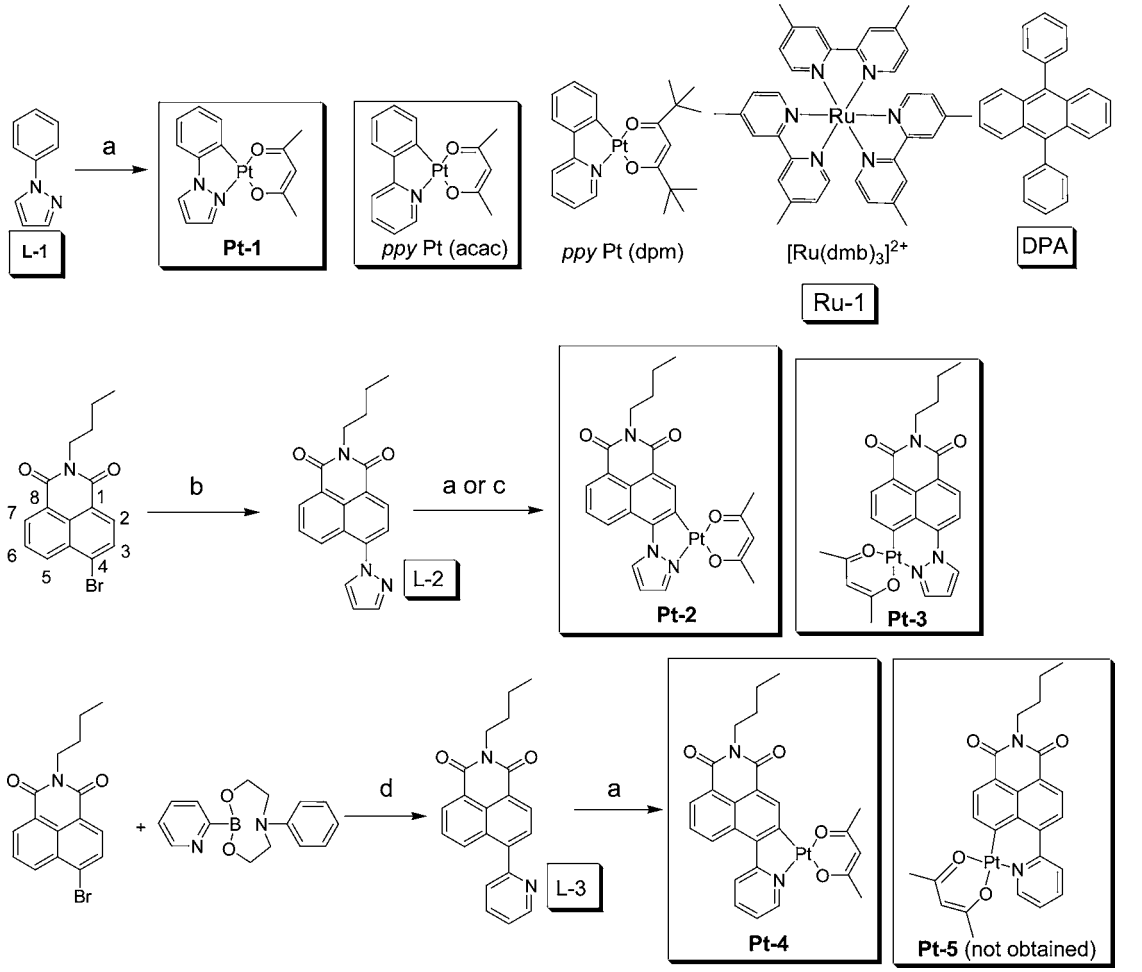

[a]The molecular structures of the triplet acceptor DPA and ruthenium(II) complex $[Ru(dmb)_3][PF_6]_2$ (**Ru-1**) used in upconversion are also shown. (a) (i) K_2PtCl_4, 2-ethoxyethanol/water (3:1, v/v), Ar, 80 °C, 16 h; (ii) Hacac/Na_2CO_3, 2-ethoxyethanol, Ar, 100 °C, 16–20 h. (b) Pyrazole, acetonitrile/toluene, Cs_2CO_3, EDTA·2Na, CuI, Ar, reflux 24 h. (c) (i) K_2PtCl_4, 2-ethoxyethanol/water (3:1, v/v), Ar, microwave, 0.5 h; (ii) Hacac/Na_2CO_3, 2-ethoxyethanol, Ar, microwave, 0.5 h. (d) $Pd(PPh_3)_4$, K_2CO_3, CuI, MeOH/toluene, Ar, reflux, 8 h.

with the five-membered coordination ring was observed (**Pt-4**). With density functional theory (DFT) optimization of the geometry of the complexes (see a later section), we found that the isomer with the six-membered coordination center (**Pt-5**) is destabilized by ca. 16.3 kJ mol^{-1} more than **Pt-4**. We found that the yield of **Pt-3** can be significantly improved by using microwave irradiation.[21,23,24]

2.2. UV–Vis Absorption of the Ligands and Cyclometalated Complexes. UV–vis absorption of the C^N ligands **L-1**, **L-2**, and **L-3** was studied (Figure 1a). 1-Phenylpyrazole gives absorption at 256 nm because of the small size of the π-conjugation framework. For NI-containing **L-2** and **L-3**, however, a strong absorption at 353 nm was observed (ε = 15 200 M^{-1} cm^{-1} for **L-2**).

With cyclometalation, generally absorption at a more red-shifted region was observed for complexes containing the NI moiety (ca. 443 nm and ε = 21 900 M^{-1} cm^{-1} for **Pt-3**; Figure 1b). For the complex with the phenylpyrazole ligand (**Pt-1**), however, absorption is located at a much shorter wavelength (314 nm). For [ppyPt(acac)], absorption is at 410 nm (ε = 3700 M^{-1} cm^{-1}). The new complexes show a red-shifted absorption compared to the NI-containing platinum(II)

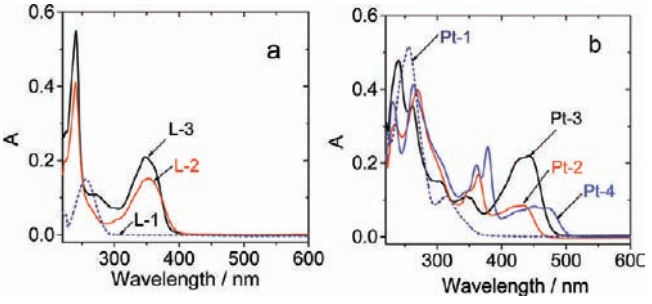

Figure 1. (a) UV–vis absorption of the ligands **L-1**, **L-2**, and **L-3**. (b) UV–vis absorption of the platinum(II) complexes **Pt-1**, **Pt-2**, **Pt-3**, and **Pt-4**. c = 1.0 × 10^{-5} M in CH_2Cl_2 at 25 °C.

complexes reported by us previously (**Pt-9**, **Pt-10**, and **Pt-11**; Scheme 1).[8,19,20]

Interestingly, absorption of the complex with a six-membered coordination ring (**Pt-3**) gives a much stronger absorption at 443 nm (ε = 21 900 M^{-1} cm^{-1}) than the isomer with a five-membered coordination ring (**Pt-2**; ε = 7164 M^{-1} cm^{-1}). The detail mechanism for this different absorption is unclear.

dx.doi.org/10.1021/ic201254w | Inorg. Chem. 2011, 50, 11446–11460

However, our DFT/time-dependent DFT (TDDFT) calculations clearly predict a stronger absorption for **Pt-3** than for **Pt-2** (by the oscillator strength of the transitions; see later sections). It should be pointed out that UV−vis absorption of **Pt-2**, **Pt-3**, and **Pt-4** is red-shifted compared to the normal cyclometalated platinum(II) complexes.[21,23] Thus, the present strategy with NI as the C donor of the C^N ligand (i.e., direct cyclometalation of the organic chromophores) is a promising method for accessing the transition-metal complexes with the light-harvesting ability.

2.3. Photoluminescence of the Cyclometalated Platinum(II) Complexes: RT Phosphorescence of NI. All of the complexes containing the NI moiety show RT red phosphorescence in solution (Figure 2). **Pt-1** is nonphosphorescent at RT. This lack of phosphorescence may be due to its unique acac-localized triplet excited state (see the DFT Calculations section).

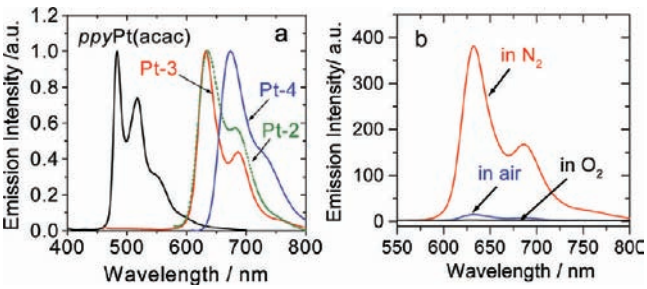

Figure 2. (a) Emission of ppyPt(acac) (λ_{ex} = 345 nm), **Pt-2** (λ_{ex} = 444 nm), **Pt-3** (λ_{ex} = 456 nm), and **Pt-4** (λ_{ex} = 475 nm). c = 1.0 × 10^{-5} M in CH_2Cl_2 at 25 °C (b) Emission of **Pt-3** under N_2, air, and O_2 atmospheres (λ_{ex} = 456 nm). c = 1.0 × 10^{-5} M in CH_2Cl_2 at 25 °C.

For the platinum(II) complexes with 4-pyrazole/NI ligands, i.e., **Pt-2** and **Pt-3**, emission at 630 nm is observed (Figure 2a). The emission is greatly red-shifted compared to [ppyPt(acac)] (λ_{em} = 486 nm).[23] The emission wavelength and vibrational progression are similar to those of the ^{3}IL emission profiles of NI in the cyclometalated platinum(II) complex or N^N platinum(II) bis(acetylide) complexes.[8,19,20] For the normal cyclometalated platinum(II) complexes, the phosphorescence lifetime is usually less than 5.0 μs.[1,23] For **Pt-2** and **Pt-3**, however, phosphorescence lifetimes of 12.8 and 61.9 μs were observed, respectively.

For **Pt-4** with the NI/pyridine ligand, a red-shifted emission at 674 nm was observed (Figure 2a). We propose that this red-shifted emission is due to the pyridine moiety being more electron deficient than the pyrazole moiety; thus, the highest occupied molecular orbital (HOMO)−lowest unoccupied molecular orbital (LUMO) energy gap of **Pt-4** (3.15 eV) is smaller than that of **Pt-3** (3.28 eV). A much lower phosphorescence quantum yield of 0.2% was observed for **Pt-4**, and the lifetime was 1.3 μs. The radiative decay rate constants of the emissive complexes do not show any clear trend (Table 1).

We investigated the sensitivity of the emission intensity of **Pt-3** toward O_2 (Figure 2b). The emission is drastically quenched in an aerated solution compared to that under a N_2 atmosphere. The phosphorescence of **Pt-2** and **Pt-4** is also sensitive to O_2 (see Figure S19 in the Supporting Information).

Among the NI-containing complexes, **Pt-10** shows the largest k_r value (7.0 × 10^3 s^{-1}).[8] This was followed by **Pt-2** (k_r = 2.4 × 10^3 s^{-1}). For the nonradiative decay constant, **Pt-2** shows the largest value, k_{nr} = 8.0 × 10^4 s^{-1}. For the complex with a long T_1 excited-state lifetime and a high phosphorescence quantum yield, such as **Pt-10**, however, the k_r value (7.4 × 10^3 s^{-1}) is close to the k_{nr} value (3.0 × 10^4 s^{-1}). Furthermore, we found that the phosphorescence quantum yields followed the energy gap law; that is, the complex with a longer emission wavelength gives a lower phosphorescene quantum yield; for example, **Pt-4** gives an emission of 674 nm with a very low phosphorescence quantum yield (Φ_P) of 0.2%. Conversely, **Pt-10** emits at a much shorter wavelength (538 nm), but the phosphorescence quantum yield is much higher (Φ_P = 18.2%) (Table 1). We also noted that the vibrational spacings of the two emission bands of the complexes are different (Figure 2).[8]

We reported a N^N platinum(II) bis(acetylide) complex with the ethynylene/NI ligand,[20] which shows an emission band at 621 nm with a lifetime of 124 μs and was assigned to the ^{3}IL emission of the NI moiety with the transient absorption studies.[20] **Pt-2** and **Pt-3** show similar emission profiles (wavelength and vibrational progression), which is an indication of ^{3}IL emission of the NI group. The principal photophysical properties of the complexes are summarized in Table 1. The radiative decay rate constants (k_r) and the nonradiative decay rate constants (k_{nr}) were calculated (Table 1). For the NI-containing complexes, the k_r is small, on the 10^3

Table 1. Photophysical Parameters of the Ligands and Platinum Complexes

	λ_{abs}[a]/nm	λ_{em}/nm	Φ_F[b]	Φ_P[c]	τ[d]	$k_r^f/10^4$ s^{-1}	$k_{nr}^f/10^6$ s^{-1}
L-1	256 (1.49)	311	0.019	[e]	1.8 ns	1055	545.00
L-2	240 (4.12), 353 (1.52)	433	0.631	[e]	4.3 ns	14 674	85.81
L-3	241 (0.55), 347 (0.21)	408	0.124	[e]	5.1 ns	2431	171.76
Pt-1	256 (5.15), 314 (1.10)	[e]	[e]	[e]	[e]	[e]	[e]
Pt-2	270 (3.98), 364 (1.69), 434 (0.85)	636	[e]	0.035	12.8 μs	0.27	0.08
Pt-3	240 (4.79), 261 (3.55), 345 (1.09), 443 (2.19)	632	[e]	0.052	61.9 μs	0.08	0.02
Pt-4	263 (4.14), 379 (2.45), 360 (1.95), 452 (0.82)	674	[e]	0.002	1.3 μs	0.15	0.77
Pt-9	243 (5.20), 296 (2.38), 390 (3.37)	638	[e]	0.011	6.6 μs	0.17	0.15
Pt-10	240 (5.46), 293(2.28), 336 (2.32), 357 (1.73), 400 (0.41)	538	[e]	0.182	25.5 μs	0.71	0.03

[a]Extinction coefficients (10^4 M^{-1} cm^{-1}) are shown in parentheses. [b]Fluorescence quantum yield with quinine sulfate as the standard (Φ_F = 0.547 in 0.05 M sulfuric acid). [c]Phosphorescence quantum yield in CH_2Cl_2 with Ru(Phen)(bpy)$_3$ as the standard (Φ_P = 6.0% in MeCN). [d]Fluorescence lifetimes (in ns) or lifetimes of the triplet excited state (measured by transient absorption, in μs). [e]Not applicable. [f]Radiative deactivation rate constant (k_r) and nonradiative deactivation rate constant (k_{nr}). $k_r = \Phi_{em}/\tau_{em}$; $k_{nr} = (1 - \Phi_{em})/\tau_{em}$. It is assumed that the emitting excited state is produced with unit efficiency.

dx.doi.org/10.1021/ic201254w | Inorg. Chem. 2011, 50, 11446–11460

s^{-1} scale; this is an indication for the long-lived ^{3}IL excited state.

2.4. Emission Spectra of the Complexes at 77 K. In order to study the emissive excited state of the complexes, the emission spectra at 77 K and RT were compared (Figure 3). It is known that the ^{3}MLCT emissive excited state usually gives a large thermally induced Stokes shift (ΔE_S); that is, the emission spectra at low temperature will show a blue shift compared to the emission at RT.[30,31] **Pt-1** is nonphosphorescent at RT. At 77 K, however, a structured emission at 400−500 nm was observed. For **Pt-3** and **Pt-4**, very small thermally induced Stokes shifts of 51 and 266 cm^{-1} were observed, respectively. The ΔE_S value of **Pt-2** is extremely small, indicating a ^{3}IL feature for the T_1 excited state of the complexes. The vibrational progression of the emission spectra became more significant at 77 K, which is the feature of the ^{3}IL excited-state emission. Thus, 77 K emission spectra demonstrated the ^{3}IL emission (see the DFT Calculations section).

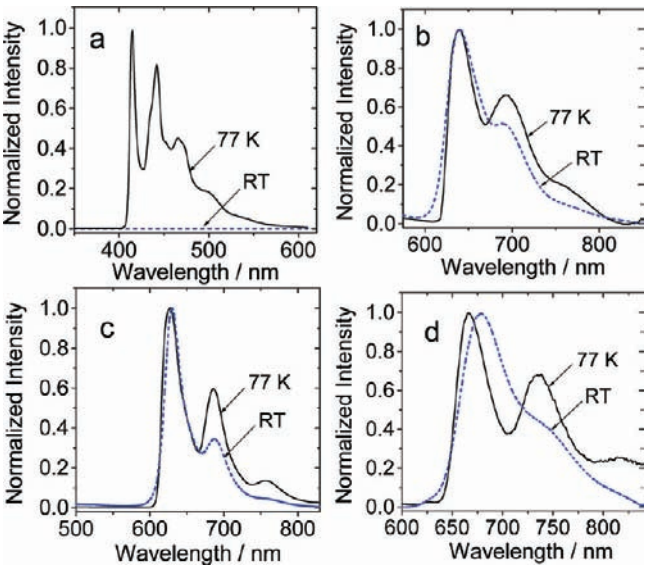

Figure 3. Photoluminescence spectra of **Pt-1** (λ_{ex} = 314 nm), **Pt-2** (λ_{ex} = 438 nm), **Pt-3** (λ_{ex} = 455 nm), and **Pt-4** (λ_{ex} = 479 nm) at RT (in EtOH/MeOH, 4:1, v/v) and 77 K (in EtOH/MeOH, 4:1, v/v).

2.5. Polarity Dependency of the Electronic Spectroscopy. UV−vis absorption and the phosphorescence spectra of the complexes were studied in solvents with different polarities (Figure 4). It is known that charge-transfer-related absorption and emission usually show shifts with variation of the solvent polarity. We do not observe any drastic shift of the UV−vis absorption of the complexes. Thus, absorption of the complexes in the low-energy region of the spectra is due to ^{1}IL absorption. For phosphorescence emission, no shift of the emission peak was observed by variation of the solvents. Thus, we propose that the emissions of the NI-containing complexes are due to the ^{3}IL excited state. Previously, it was shown that ^{3}MLCT emission will show solvent-polarity-dependent emission, and usually the emission band will move to a longer wavelength by increasing the polarity of the solvents.[32]

2.6. Redox Behavior. The electrochemical properties of the complexes were examined by cyclic voltammetry (Figure 5), and the redox data are compiled in Table 2. The ligands exhibit reversible and irreversible reduction waves at around −1.50 and −2.14 V vs $Ag/AgNO_3$ in CH_2Cl_2, respectively. **Pt-1** shows a reversible oxidation wave near 0.57 V vs $Ag/AgNO_3$, which is similar to those of other platinum complexes.[22,23,28] Similarly, the [ppyPt(dpm)] complex (dpm = dipivolylmethane, i.e., 2,2,6,6-tetramethyl-3,5-heptanedione; Scheme 1) is reported to have a reversible reduction at −2.6 V and an irreversible oxidation at +0.51 V in a *N*,*N*-dimethylformamide solution, and it is generally considered that reduction is localized on the C^N ligand and oxidation is localized on the metal center for these cyclometalated complexes at the ground state.[22,23] Therefore, reduction can be assigned to the C^N ligand, and oxidation can be assigned to the metal center at the ground state.[22,23,28]

2.7. Nanosecond Time-Resolved Transient Difference Absorption Spectra. Nanosecond transient difference absorption spectroscopy (laser photolysis) can be used for the study of the triplet excited state of the complexes.[8,18,33−37]

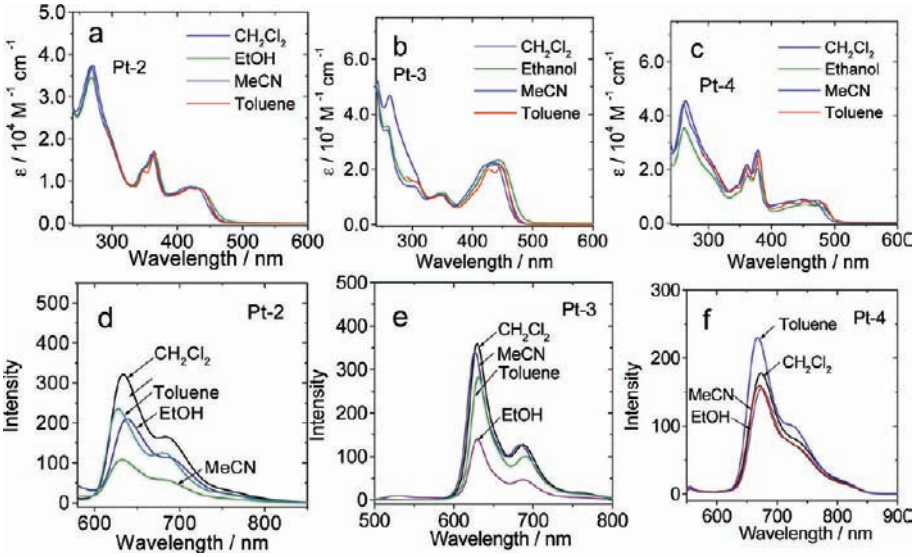

Figure 4. Absorption spectra of (a) **Pt-2**, (b) **Pt-3**, and (c) **Pt-4** and emission spectra of (d) **Pt-2**, (e) **Pt-3**, and (f) **Pt-4**. $c = 1.0 \times 10^{-5}$ M in CH_2Cl_2, EtOH, MeCN, and toluene, respectively. The emission spectra were measured under a N_2 atmosphere at 25 °C.

dx.doi.org/10.1021/ic201254w | Inorg. Chem. 2011, 50, 11446−11460

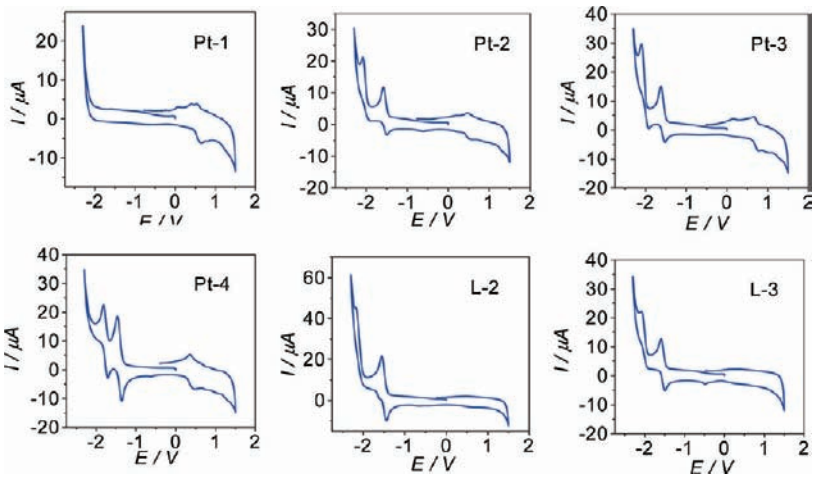

Figure 5. Cyclic voltammograms of platinum complexes and their ligands in nitrogen-purged CH_2Cl_2. 0.5 mM complex in 0.1 M n-Bu_4NPF_6/CH_2Cl_2 at a scan rate of 100 mV s^{-1} at 25 °C.

Table 2. Electrochemical Data of the Platinum(II) Complexes and Ligands

	E_{ap} or $E_{1/2}$ (V)	E_{cp} or $E_{1/2}$ (V)
Pt-1	0.57	−0.30 (irr)
Pt-2	0.50	−1.54, −2.09 (irr)
Pt-3	0.72	−1.56, −2.10 (irr)
Pt-4	0.39	−1.41, −1.76
L-2		−1.50, −2.14 (irr)
L-3		−1.54, −2.08 (irr)

Recently, we reported the first example of RT phosphorescence of the NI group with a platinum(II) bis(acetylide) complex.[20] The transient of the N^N platinum bis(naphthalimideacetylide) complex shows the characteristic triplet absorption feature of the NI moiety.[20]

The transient absorption spectra of the complexes are presented (Figure 6). No transient absorption can be obtained for **Pt-1**, probably because of its short excited-state lifetime (the maximal resolution of our time-resolved spectrometer is nanoseconds). Transient absorption in the 500−700 nm region was observed for **Pt-3**. These features are similar to those of the NI-localized ^{3}IL excited state,[20] and they are drastically different from the transient absorption features of [ppyPt(acac)]. Bleaching at ca. 370 nm was observed. For **Pt-2** and **Pt-4**, no significant ground-state bleaching at 450 nm was observed, which is probably due to the strong transient absorption in the region. This is supported by bleaching at shorter wavelength such as ca. 370 nm. This assignment is supported by the TDDFT calculations, which predicted absorption for the T_1 state at ca. 400 nm. The negative signals between 700 and 750 nm for **Pt-2** and **Pt-4** are due to emission of the complexes, as opposed to ground-state bleaching, which were found at 356, 434, or 360 nm for **Pt-2**, **Pt-3**, or **Pt-4**, respectively.

Pt-3 shows no strong absorptions at 370 nm in steady-state UV−vis absorption (Figure 1b). Furthermore, TDDFT calculations predict absorption beyond 800 nm for **Pt-2** and **Pt-4** but not for **Pt-3**. These predictions are in agreement with the experiments. The calculations predict transient absorption in the regions of 500 and 600 nm, which is supported by the experimental results. Transient absorption at 410, 536, 645, and 791 nm was observed. This can be fully rationalized by TDDFT calculations on the transitions between the triplet excited states, such as $T_1 \rightarrow T_2$, etc. The calculations predict absorption bands of the T_1 state for **Pt-4** at 423 nm (f = 0.1960, $T_1 \rightarrow T_{18}$), 535 nm (f = 0.1774, $T_1 \rightarrow T_{12}$), 651 nm (f = 0.0658, $T_1 \rightarrow T_6$), and 806 nm (f = 0.0298, $T_1 \rightarrow T_4$). The intensive absorption of the T_1 state at 423 nm may be responsible for the absence of bleaching of the ground state at ca. 450 nm.

Herein, the quantum yields (Φ_T) of the triplet excited states of the complexes were determined by a comparative method (please note this is not the phosphorescence quantum yield).[38a] Biphenyl ketone was used in the actinometer (Φ_T = 1.00; the triplet molar extinction coefficient at 530 nm was 7220 ± 320 M^{-1} cm^{-1}).[38b] Φ_T = 0.62 was observed for **Pt-3**, while the Φ_T values of **Pt-2** and **Pt-4** are 0.46 and 0.36, respectively. Φ_T of the six-membered chelate ring (**Pt-3**) is higher than that of the five-membered chelate rings (**Pt-2** and **Pt-4**).

2.8. DFT Calculations: Rationalization of the Electronic Spectra and the ^{3}IL Excited States. Previously, we studied the platinum(II) naphthalimideacetylide complexes and platinum(II) complexes with the NI moiety tangled on the ppy ligands as well as ruthnium(II) polyimine complexes.[8,18−20,38]

First, the geometries of the complexes were optimized (Figure 7). For **Pt-1**, the phenyl and pyrazole moieties are coplanar; the dihedral angle of the two subunits is 0°. For **Pt-2**, the dihedral angle between the NI and pyrazole moieties is 7.7°, and the dihedral angle between the acac−Pt plane and the NI unit is 0.2°. A more distorted geometry was found for **Pt-3**, for which the dihedral angle between the NI and pyrazole moieties is 24.8°. Furthermore, the dihedral angle between the acac−Pt plane and the NI unit is 16.4°. Interestingly, for the 4-pyridine/NI ligand, only the five-membered isomer (**Pt-4**) was obtained; no six-membered ring was obtained (**Pt-5**). For **Pt-4**, the dihedral angle between the NI and pyrazole moieties is 10.3°. The dihedral angle between the acac−Pt plane and the NI unit is 2.2°. We also investigated the geometry of the expected isomer **Pt-5**. The dihedral angle between the pyridine and the NI unit is 29.2°. A significant distortion was found for the coordination center; the dihedral angle between the acac−Pt plane and the NI unit is 23.2° (see Figure S21 in the Supporting Information). The significant deviation from the planar geometry may make **Pt-5** unstable.

Pt-5 was not obtained in the preparation of the complexes; we compared the energy of the different isomers. For **Pt-2** and **Pt-3**, the energetic difference is only 4.9 kJ mol^{-1}. For the NI/

dx.doi.org/10.1021/ic201254w | Inorg. Chem. 2011, 50, 11446−11460

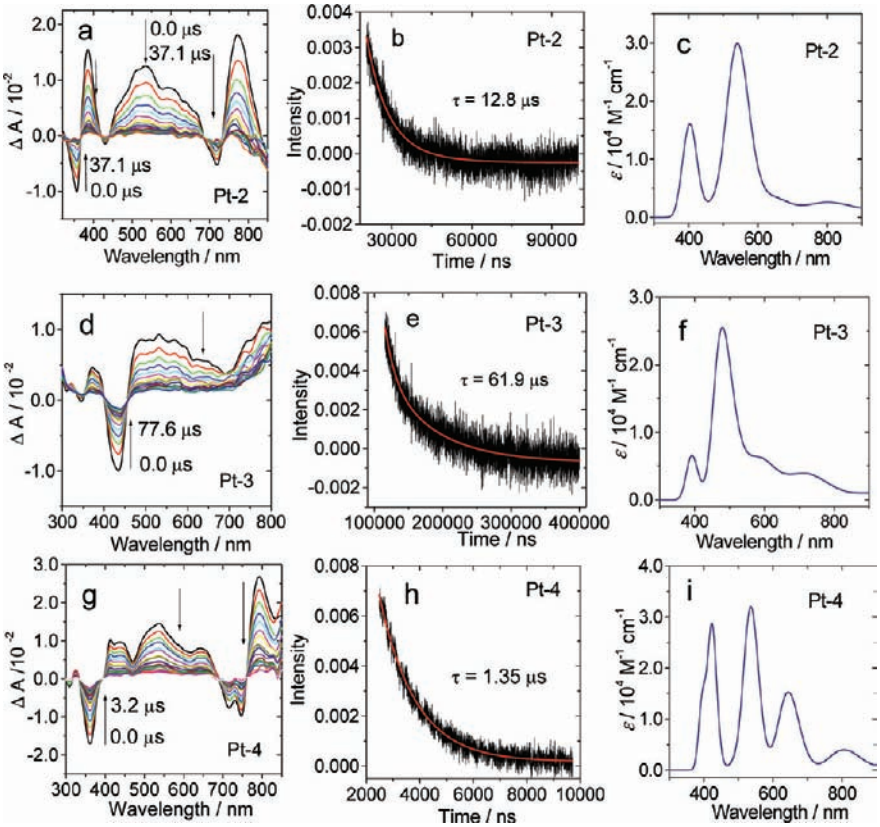

Figure 6. Nanosecond transient absorption difference spectra of the complexes. (a, d, and g) Spectra of **Pt-2**, **Pt-3**, and **Pt-4** in CH_2Cl_2 measured as a function of the delay times indicated, following 355 nm pulsed laser excitation. (b, e, and h) Lifetimes of **Pt-2** (τ_T = 12.8 μs), **Pt-3** (τ_T = 61.9 μs), and **Pt-4** (τ_T = 1.35 μs), following decay at the bleaching wavelength. c [complexes] = 5.0 × 10^{-5} M at 25 °C. (c, f, and i) Calculated transient absorption spectra. Please note that the information of bleaching cannot be obtained by TDDFT calculations. CH_2Cl_2 was used as the solvent in the calculations (PCM model).

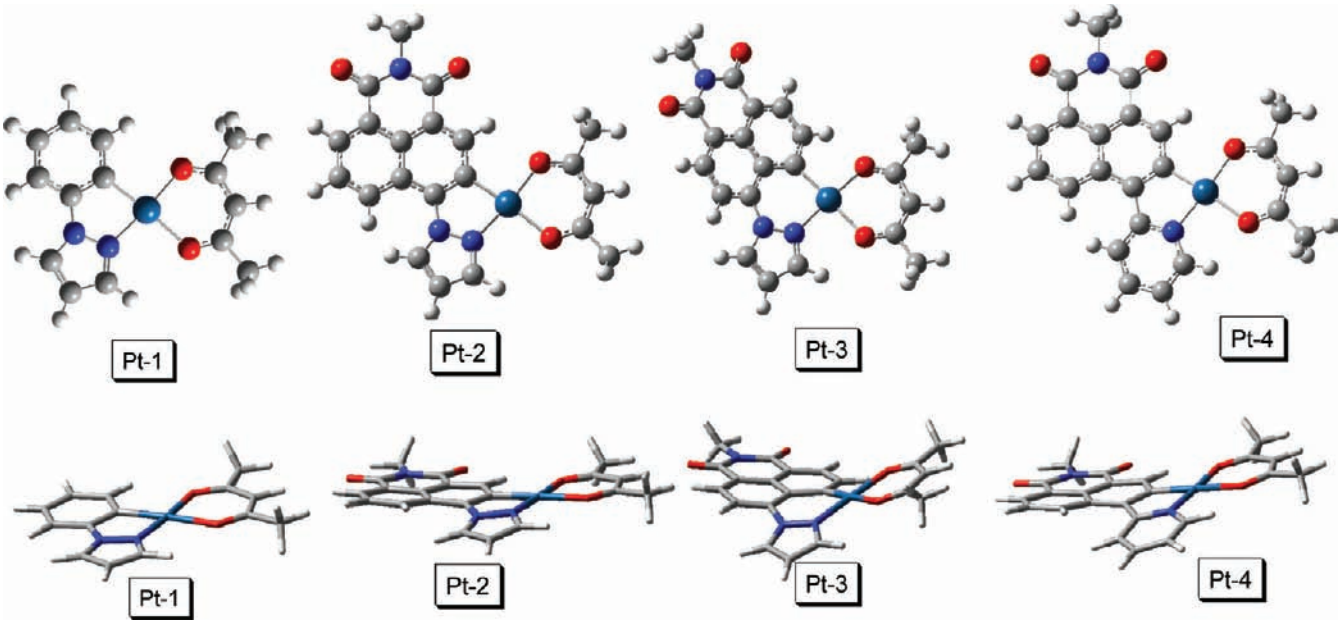

Figure 7. Optimized molecular structures of **Pt-1**, **Pt-2**, **Pt-3**, and **Pt-4**. The top (upper row) and side (lower row) views of the optimized geometries are presented to illustrate distortion of the coordination centers (among which **Pt-3** shows the most significant deviation from the coplanar geometry).

pyridine-derived complex **Pt-4** and the expected isomer **Pt-5** (not obtained in the synthesis), however, the calculated energy difference is up to 16.3 kJ mol^{-1} (**Pt-5** has higher energy than **Pt-4**); thus, we propose that **Pt-5** is thermodynamically unstable. As a result, we did not obtain this complex in the synthesis.

dx.doi.org/10.1021/ic201254w | *Inorg. Chem.* 2011, 50, 11446–11460

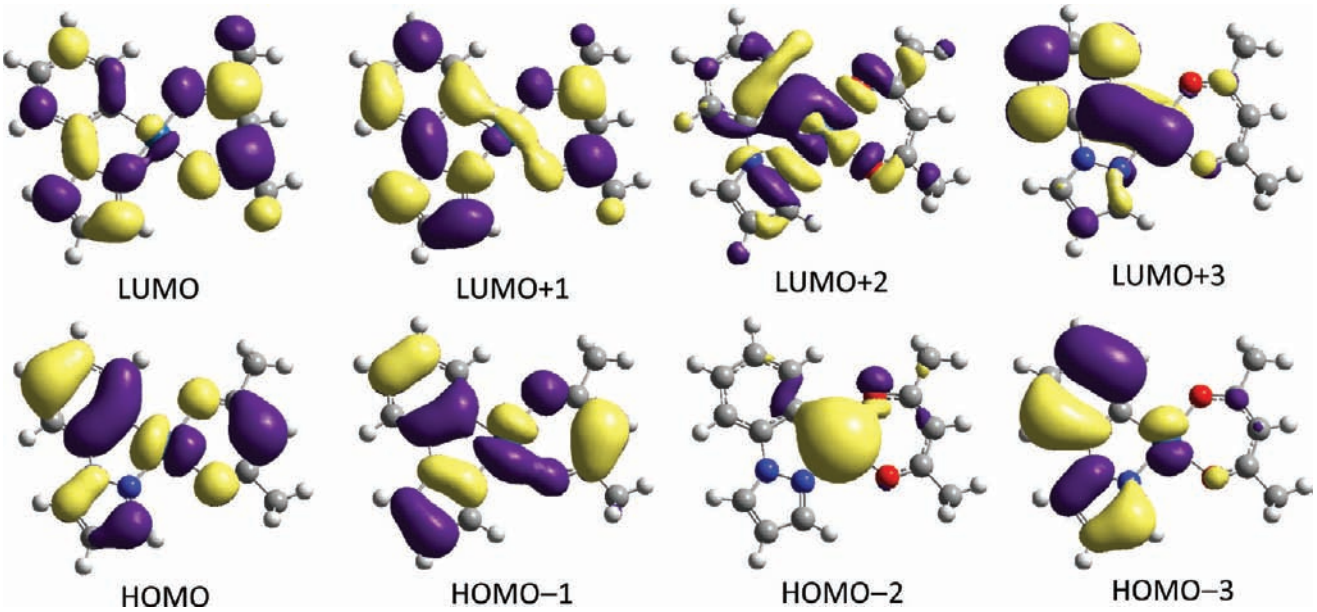

Figure 8. Electron density maps of the frontier molecular orbitals of complex **Pt-1** based on the optimized ground-state geometry. The solvent dichloromethane was considered in the calculations (PCM model). Calculated at the B3LYP/6-31G/LANL2DZ level with *Gaussian 09W*.

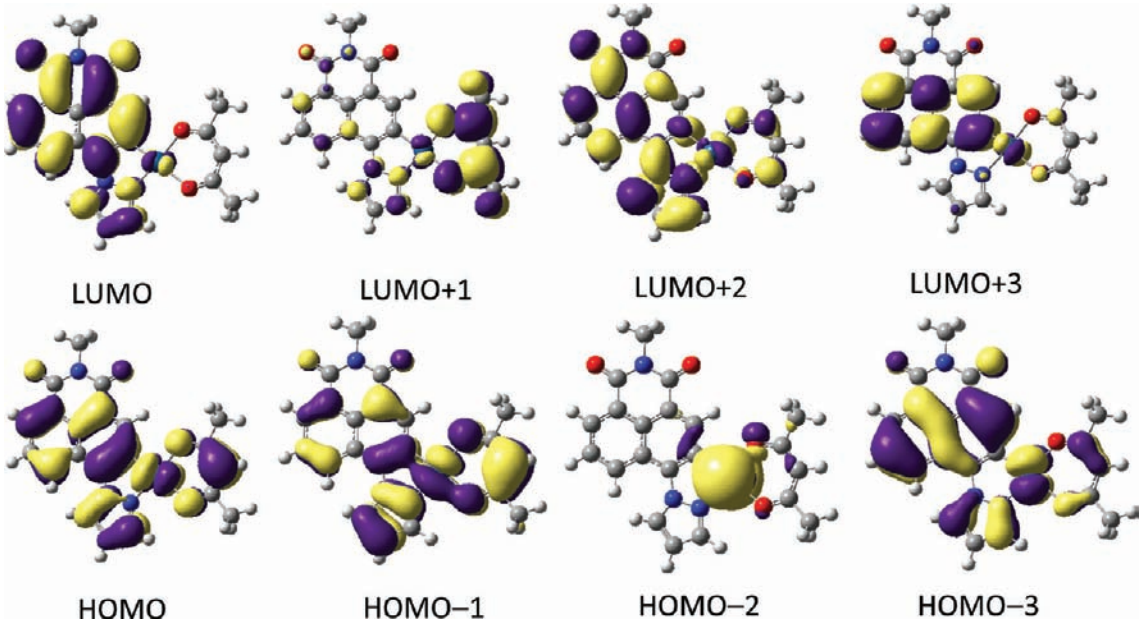

Figure 9. Electron density maps of the frontier molecular orbitals of complex **Pt-2** based on the optimized ground-state geometry. The solvent dichloromethane was considered in the calculations (PCM model). Calculated at the B3LYP/6-31G/LANL2DZ level with *Gaussian 09W*.

The molecular orbitals of **Pt-1** are present in Figure 8. The acac unit contributes significantly to both HOMO and LUMO. Furthermore, the phenyl moiety contributes to HOMO more than the pyrazole unit, and the profile is reversed for LUMO. This is in agreement with the normal cyclometalated platinum(II) complexes, in which the C donor to the C–Pt–N bond contributes to the HOMO and the N donor of the C–Pt–N bond contributes more to the LUMO.[1]

The most significant difference of the frontier molecular orbitals of **Pt-2** from that of **Pt-1** is the lack of contribution of the acac moiety to the LUMO (Figure 9). This result indicates that the NI moiety is electron-deficient and serves as an electron sink.[8,21] Thus, the LUMO is mainly localized on the NI moiety. Distribution of the LUMO on an electron-deficient moiety may decrease the energy level of the LUMO. For **Pt-2**, we found significant contribution of the NI subunit to the frontier molecular orbitals (Figure 9). Involvement of the NI subunit in the frontier molecular orbitals may suggest a ^{3}IL feature of the excited state. Similar results were found for **Pt-3** and **Pt-4** (see Figures S22 and S23 in the Supporting Information).

UV–vis absorption of the complexes was investigated with TDDFT calculations based on the optimized ground-state geometries (Franck–Condon principle; Tables 3 and 4 and S1 and S2 in the Supporting Information). The calculations predict a maximum absorption for **Pt-1** at 325 nm ($S_0 \rightarrow S_1$ transition). For the NI-containing platinum(II) complexes, however, UV–vis absorption at 438, 438, and 466 nm was

dx.doi.org/10.1021/ic201254w | *Inorg. Chem.* 2011, 50, 11446–11460

Table 3. Electronic Excitation Energies and Corresponding Oscillator Strengths (f), Main Configurations, and CI Coefficients of the Low-Lying Electronic Excited States of Complex Pt-1 Calculated by TDDFT//B3LYP/6-31G(d)/LanL2DZ Based on the Optimized Ground-State Geometries[a]

		TDDFT//B3LYP/6-31G(d)				
	electronic transition	energy[b]	f[c]	composition[d]	CI[e]	character[f]
singlet	$S_0 \rightarrow S_1$	3.82 eV, 325 nm	0.0016	H → L	0.6776	IL and MLCT
				H → L+1	0.1441	IL
	$S_0 \rightarrow S_2$	3.88 eV, 319 nm	0.0806	H−1 → L	0.2387	IL and MLCT
				H−1 → L+1	0.2232	IL and MLCT
				H → L	0.1204	IL and MLCT
				H → L+1	0.5973	IL
	$S_0 \rightarrow S_3$	4.11 eV, 301 nm	0.1887	H−1 → L	0.5558	IL and MLCT
				H−1 → L+1	0.2624	IL and MLCT
				H → L	0.3120	IL and MLCT
	$S_0 \rightarrow S_{14}$	4.98 eV, 249 nm	0.1937	H−6 → L	0.3770	
				H−5 → L+1	0.4239	
				H−4 → L	0.2841	
				H−3 → L	0.1227	LLCT and MLCT
				H−3 → L+1	0.2997	LLCT
				H → L+3	0.4501	LLCT
triplet	$S_0 \rightarrow T_1$	2.99 eV, 414 nm	0.0000[g]	H−4 → L	0.2303	
				H−4 → L+1	0.1516	
				H−1 → L	0.3155	IL and MLCT
				H−1 → L+1	0.1974	IL and MLCT
				H → L	0.4691	IL and MLCT
				H → L+1	0.2527	IL

[a] CH_2Cl_2 was used as the solvent in the calculations (PCM model). [b] Only the selected low-lying excited states are presented. [c] Oscillator strength. [d] H stands for HOMO, and L stands for LUMO. Only the main configurations are presented. [e] The coefficient of the wave function for each excitation is in absolute values. [f] IL = intraligand, LLCT = ligand-to-ligand charge transfer, and MLCT = metal-to-ligand charge transfer. [g] No spin−orbital coupling effect was considered; thus, the f values are zero.

Table 4. Electronic Excitation Energies and Corresponding Oscillator Strengths (f), Main Configurations, and CI Coefficients of the Low-Lying Electronic Excited States of Complex Pt-2 Calculated by TDDFT//B3LYP/6-31G(d)/LanL2DZ Based on the Optimized Ground-State Geometries[a]

		TDDFT//B3LYP/6-31G(d)				
	electronic transition	energy[b]	f[c]	composition[d]	CI[e]	character[f]
singlet	$S_0 \rightarrow S_1$	2.83 eV, 438 nm	0.1318	H → L	0.6976	IL and LLCT
	$S_0 \rightarrow S_4$	3.53 eV, 351 nm	0.2883	H−3 → L	0.6723	IL and MLCT
				H−1 → L	0.1202	LLCT and MLCT
				H → L	0.1983	IL and LLCT
				H → L+2	0.1077	IL and LLCT
	$S_0 \rightarrow S_{12}$	4.22 eV, 294 nm	0.1186	H−3 → L+1	0.1201	LLCT and MLCT
				H−2 → L+1	0.3080	MLCT
				H−1 → L+1	0.5347	LLCT and MLCT
				H−1 → L+2	0.1193	LLCT
				H → L+5	0.1469	
triplet	$S_0 \rightarrow T_1$	1.98 eV, 626 nm	0.0000[g]	H−3 → L	0.1675	IL and MLCT
				H−1 → L	0.2886	LLCT and MLCT
				H → L	0.6045	IL and LLCT

[a] CH_2Cl_2 was used as the solvent in the calculations (PCM model). [b] Only the selected low-lying excited states are presented. [c] Oscillator strength. [d] H stands for HOMO, and L stands for LUMO. Only the main configurations are presented. [e] The coefficient of the wave function for each excitation is in absolute values. [f] IL = intraligand, LLCT = ligand-to-ligand charge transfer, and MLCT = metal-to-ligand charge transfer. [g] No spin−orbital coupling effect was considered; thus, the f values are zero.

predicted for **Pt-2**, **Pt-3**, and **Pt-4**, respectively. Furthermore, stronger absorption for **Pt-3** than for **Pt-2** was predicted by the calculations. All of these theoretical predictions are in agreement with the experimental observations. For **Pt-1**, the electronic compositions of the lowest-lying singlet excited states are mainly the HOMO → LUMO transition. 1-Phenylpyrazole contributes significantly to the transition. The Pt atom also contributes to the transition (Table 3).

Because the emissions of the complexes were assigned as phosphorescence, the lowest-lying triplet excited states of **Pt-1** were also studied with TDDFT calculations (Table 3). The HOMO → LUMO transition is the main transition of the T_1

dx.doi.org/10.1021/ic201254w | Inorg. Chem. 2011, 50, 11446–11460

state. The TDDFT calculation predicts the ΔS_0-T_1 energy gap as 414 nm for **Pt-1**. This prediction is in good agreement with the phosphorescence emission wavelength of the complex at 77 K (395 nm; Figure 3).

The calculations predict UV−vis absorption at 438, 351, and 294 nm for **Pt-2** (Table 4). Experimentally, absorption at 434, 364, and 270 nm was observed (Figure 1b). The main contribution to the T_1 state, which is responsible for phosphorescence, is the HOMO → LUMO transition. For both orbitals, the NI contribution is significant (Figure 9). Thus, we propose that the emissive triplet excited state of **Pt-2** is featured as the ^{3}IL character. Similar results were obtained for **Pt-3** and **Pt-4** (see Tables S1, S2, S22, and S23 in the Supporting Information).

The spin-density surfaces of the complexes were also used to evaluate the triplet excited states.[25] The calculation is based on the triplet-state geometry (Figure 10). For the NI-containing

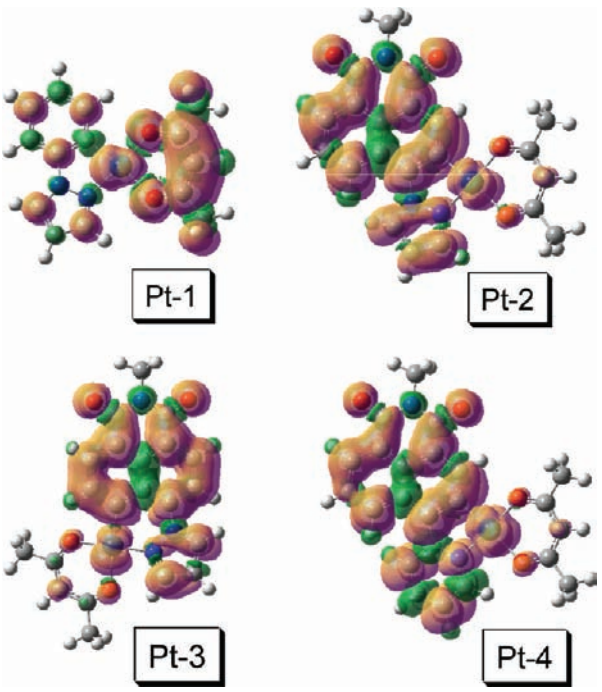

Figure 10. Spin-density surfaces for the lowest-lying triplet states of **Pt-1**, **Pt-2**, **Pt-3**, and **Pt-4**. Dichloromethane was used as the solvent in the calculations (PCM model). The calculations are based on the optimized triplet-state geometry (isovalue: ±0.0004). Calculated at the B3LYP/6-31G/LANL2DZ level with *Gaussian 09W*.

platinum(II) complexes, the spin density is localized on the NI moiety. For **Pt-1**, which gives drastically different emission properties (Figure 3), however, the spin density is mainly localized on the acac moiety. Thus, we conclude that phosphorescence of the platinum(II) complexes in which the NI moiety directly cyclometalated (**Pt-2**, **Pt-3**, and **Pt-4**) is due to the ^{3}IL excited states.

2.9. Application of the Light-Harvesting Effect and the Long-Lived ^{3}IL Excited State. Upconversion has attracted much attention because of its application in artificial photosynthesis, photocatalysis, and optical materials.[39−47] From the point of view of a chemist, a few methods are available for upconversion, for example, with nonlinear optical crystals and two-photon absorption dyes.[48,49] These methods suffer from some fundamental disadvantages, such as the requirement of an intense coherent laser for excitation (with a power density of up to MW cm^{-2}, i.e., 10^6 W cm^{-2}; note the terrestrial solar radiance power density is ca. 0.10 W cm^{-2}, AM1.5G), or the difficulty in tuning the wavelength to a value at which the upconversion materials can effectively work.

Recently, a new upconversion method based on the TTA mechanism appeared and has attracted much attention.[39] TTA-based upconversion does not require a coherent laser as the excitation source, and an excitation power density down to mW cm^{-2} is sufficient to sensitize the upconversion. Furthermore, the wavelength is at the point in which the upconversion work can be readily tuned, simply by the independent selection of the triplet donor and acceptor (but the T_1 energy levels of the donor and acceptor must be matched).

Currently, the typical triplet sensitizers used for TTA-based upconversion are the ruthenium(II) polyimine[50] and platinum-(II) porphyrin complexes.[40,41,45−47,51−55] To the best of our knowledge, few cyclometalated platinum(II) complexes have been used for TTA-based upconversion.[9]

On the basis of our previous investigation on TTA-based upconversion,[9,10,32,56,57] we propose that several photophysical properties of the sensitizer are crucial for TTA upconversion. The first is the *light-harvesting effect* of the sensitizer. Absorption at long wavelength with a high molar extinction coefficient and efficient intersystem crossing (ISC) is desired because, under these circumstances, the triplet excited states of the sensitizers can be efficiently produced upon photo-excitation. The second is the *lifetime of the triplet excited state* of the sensitizer. Sensitizers with long-lived T_1 excited states will have more of a chance to encounter an acceptor (quencher) to facilitate the triplet−triplet energy-transfer (TTET) process, by which the triplet excited state of the triplet acceptor is populated.

First, phosphorescence of the complexes with laser excitation at 473 nm was studied (Figure 11a). $[Ru(dmb)_3][PF_6]_2$ (τ_P =

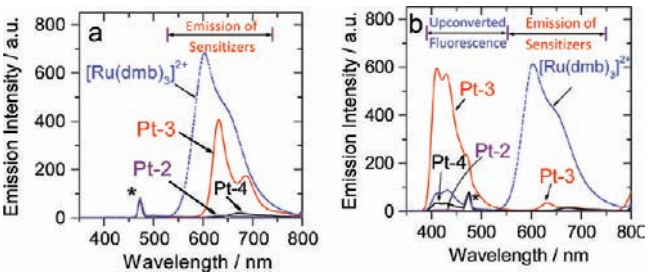

Figure 11. (a) Emission profile of **Pt-2**, **Pt-3**, **Pt-4**, and $[Ru(dmb)_3][PF_6]_2$ (1.0×10^{-5} M). Excitation by a blue laser (λ_{ex} = 473 nm, 5 mW). (b) Emission of the upconverted fluorescence of DPA (4.3×10^{-5} M) and the residual phosphorescence of **Pt-2**, **Pt-3**, **Pt-4**, and (**Ru-1**) in the upconversion experiments. The asterisks denote the scattered laser at 473 nm at 25 °C.

0.8 μs) was included for comparison. $[Ru(dmb)_3][PF_6]_2$ shows the most intense emission.[53] **Pt-3** shows intense emission because of its high quantum yield and absorption in the visible region. Other complexes studied herein give much weaker emission because of the lower quantum yield or poor absorption at 473 nm compared to **Pt-3**.

Next, we investigated emission of the complexes in the presence of a triplet acceptor/annihilator, 9,10-diphenylanthracene (DPA), which shows perfect photostability and a high fluorescence quantum yield (Φ_F = 0.95), as well as an

dx.doi.org/10.1021/ic201254w | *Inorg. Chem.* 2011, 50, 11446−11460

appropriate T_1 state energy level. Anthracene was not used because of its much lower fluorescence quantum yield (Φ_F = 0.27).

In the presence of DPA, significant blue emission was observed in the region of 400−500 nm for **Pt-3**. Irradiation of **Pt-3** or DPA alone does not produce this emission band; thus, the blue emission in the region of 400−500 nm was assigned to the upconverted emission of DPA. The anti-Stokes shift is 0.48 eV. Much weaker blue emission was observed for other complexes. Phosphorescence of **Pt-3** is almost completely quenched (Figure 11b).

Upconversion is significant for the unaided eye (Figure 12). For the sensitizers alone, **Pt-3** gives red phosphorescence with a

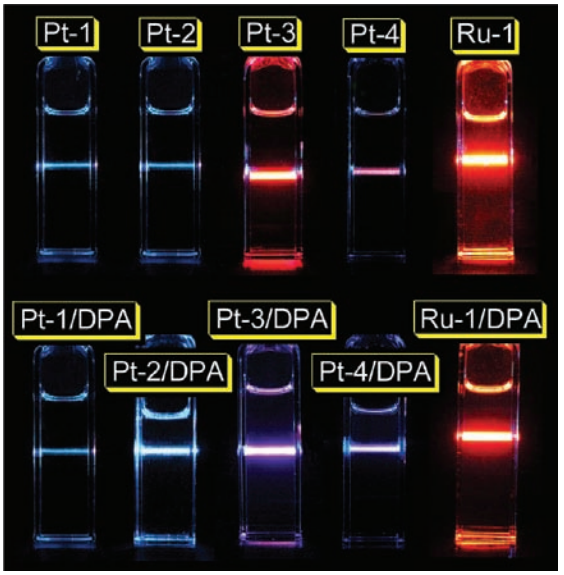

Figure 12. Upconversion with the complexes as triplet sensitizers and DPA as the triplet acceptor. The result of $[Ru(dmb)_3][PF_6]_2$ is included for comparison. Photographs of phosphorescence and upconversion of the complex sensitizers. Excited by a blue laser (λ_{ex} = 473 nm, 5 mW) at 25 °C.

473 nm laser excitation and the emission of **Pt-4** is deep red. For **Pt-1** and **Pt-2**, no significant emission was observed and the light paths in the vials of **Pt-1** and **Pt-2** are due to scattering of the excitation laser beam (473 nm). With the addition of DPA into the solutions, significant upconversion was observed for **Pt-3** (the color of the beam path changed from red to purple). Upconversion was also observed with **Pt-4**, but to a minor extent. No significant upconversion was observed with $[Ru(dmb)_3][PF_6]_2$.

An upconversion quantum yield Φ_{UC} of up to 14.1% was observed for **Pt-3**. We noticed that a recently reported upconversion with the platinum(II) acetylide complex gave an upconversion quantum yield of less than 1.5%.[47] Upconversion quantum yields higher than 11.1%, a value thought to the maximum limit, is reasonable because recently it was realized that encounters other than the singlet/ground state can give singlet emission.[39,55] By comparison, $[Ru(dmb)_3][PF_6]_2$ gives an upconversion quantum yield of only 0.5% (Table 5). The difference in the values is due to the light-harvesting ability and lifetime of triplet excited states. **Pt-3** and $[Ru(dmb)_3][PF_6]_2$ show a molar extinction coefficients (ε) of 3853 and 14 424 M^{-1} cm^{-1} at 473 nm, respectively. The triplet

Table 5. Luminescent Lifetimes (τ), Stern−Volmer Quenching Constants (K_{SV}), Bimolecular Quenching Constants (k_q), Relative Fluorescence Emission Intensities (I_F), and Upconversion Quantum Yields (Φ_{UC}) of the Pt-2, Pt-3, Pt-4, and $[Ru(dmb)_3]^{2+}$ (Ru-1) Complexes in a Deaerated CH_2Cl_2 Solution at 25 °C

	τ^a /μs	$K_{sv}{}^b/M^{-1}$ (10^3)	$k_q{}^c/M^{-1}\ s^{-1}$ (10^9)	$r^{2\ d}$	$I_F{}^e$	$\Phi_{UC}{}^f$/ %
Pt-2	12.8	124.6	8.40	0.99	*g*	*g*
Pt-3	61.9	307.0	5.11	1.00	8.1	14.1
Pt-4	1.26	4.8	3.89	1.00	0.4	0.3
Ru-1	0.80	3.9	4.88	0.98	1.0	0.5

[a]Luminescent lifetimes (τ). [b]Stern−Volmer quenching constants (K_{SV}) of the quenching of phosphorescence of platinum complexes by the triplet acceptor DPA. [c]Bimolecular quenching constants (k_q). [d]Determination coefficients of the quenching constants. [e]Relative upconverted fluorescence emission intensity, with the upconversion emission intensity of $[Ru(dmb)_3]^{2+}$ as the standard. [f]Upconversion quantum yield. [g]Too low to be determined accurately.

excited state of **Pt-3** (τ = 61.9 μs) is much longer than the lifetime of $[Ru(dmb)_3][PF_6]_2$ (τ = 0.8 μs).

In order to study the efficiency of the TTET process, Stern−Volmer quenching curves were constructed (Figure 13). We

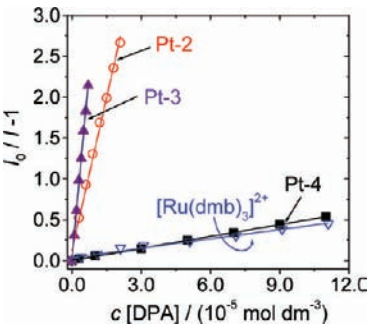

Figure 13. Stern−Volmer plots generated from the phosphorescence intensity quenching of complex $[Ru(dmb)_3][PF_6]_2$ (λ_{ex} = 473 nm), **Pt-2** (λ_{ex} = 444 nm), **Pt-3** (λ_{ex} = 473 nm), and **Pt-4** (λ_{ex} = 473 nm) as a function of the DPA concentration. 1.0 × 10^{-5} M in CH_2Cl_2 at 25 °C.

found significant quenching effects for **Pt-2** and **Pt-3** in the presence of DPA. The Stern−Volmer quenching constants were calculated as K_{SV} = 1.25 × 10^5 M^{-1} and K_{SV} = 3.07 × 10^5 M^{-1} for **Pt-2** and **Pt-3**, respectively. For **Pt-4** and $[Ru(dmb)_3][PF_6]_2$, however, much weaker quenching effects were observed; their Stern−Volmer quenching constants are ca. 75 times smaller than those of **Pt-3** (Table 5). The quenching constants are in line with the lifetime of the T_1 state of the complexes. Longer triplet excited-state lifetimes will produce an efficient TTET process. We noticed that a large K_{SV} value was observed for **Pt-2**, but no significant upconversion was observed for **Pt-2** (Figure 11). We attribute this result to the poor absorption of **Pt-2** at 473 nm; thus, the concentration of the sensitizers at the triplet state is under the threshold for significant upconversion. Thus, both the light-harvesting and lifetime of the T_1 state of the sensitizers (complexes) are crucial for efficient upconversion.

It should be pointed out that the quenching constants of **Pt-2** and **Pt-3** are up to 30-fold of a recently reported platinum(II) acetylide complex.[47] The K_{SV} value of **Pt-3** is 60-fold of that of

dx.doi.org/10.1021/ic201254w | Inorg. Chem. 2011, 50, 11446−11460

Scheme 3. Qualitative Jablonski Diagram Illustrating the Sensitized TTA Upconversion Process between Platinum(II) Complexes (Exemplified by Pt-3) and the Triplet Acceptor DPA[a]

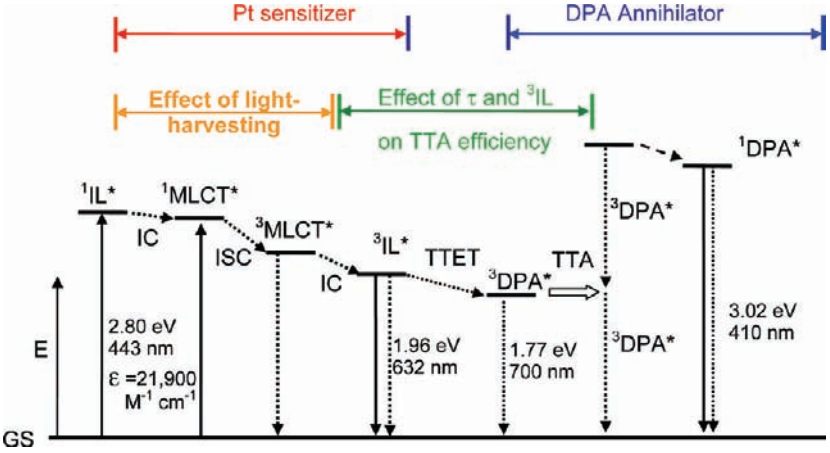

[a]The effect of the light-harvesting ability and luminescence lifetime of the platinum(II) sensitizer on the efficiency of TTA-based upconversion is also shown. *E* is energy. GS is the ground state (S_0). ^{1}IL* is the intraligand singlet excited state (NI localized). IC is inner conversion. ISC is intersystem crossing. ^{3}MLCT* is the platinum(II)-based metal-to-ligand charge-transfer triplet excited state. ^{3}IL* is the intraligand triplet excited state (NI localized). TTET is triplet−triplet energy transfer. ^{3}DPA* is the triplet excited state of DPA. TTA is triplet−triplet annihilation. ^{1}DPA* is the singlet excited state of DPA. The emission band observed for the sensitizers alone is the ^{3}IL emissive excited state. The emission bands observed in the TTA experiment are the simultaneous ^{3}IL* emission (phosphorescence) and the ^{1}DPA* emission (fluorescence).

$Ir(ppy)_3$, a cyclometalated complex that was used for TTA-based upconversion.[46]

The mechanism of the TTA-based upconversion with platinum(II) complexes (exemplified by **Pt-3**) can be summarized in Scheme 3.[39,41] First, the triplet sensitizers are populated with photoexcitation. Direct excitation of the ligand or ^{1}MLCT will lead to population of the singlet excited state. With the heavy-atom effect of the Pt^{II} ion, the $S_1 \rightarrow T_1$ ISC will lead to a ^{3}IL excited state. Please note that the ^{3}IL excited state shows a much longer lifetime than the normal ^{3}MLCT state. Thus, the efficiency of the TTET process will be improved.[9] Annihilation of the triplet excited state will produce the singlet excited state, and singlet emission (fluorescence) will be observed. Note that the wavelength of upconverted fluorescence is shorter than the initial photoexcitation wavelength. It should be pointed out that the light-harvesting and long-lived ^{3}IL triplet excited state of **Pt-3** make it an ideal triplet sensitizer for TTA-based upconversion, excited with low-power light (70 mW cm^{-2}). Under our experimental conditions, the lowest excitation power density that can produce upconversion is 22.4 mW cm^{-2}.

3. CONCLUSION

In conclusion, we prepared cyclometalated platinum(II) complexes (**Pt-2**, **Pt-3**, and **Pt-4**) in which the NI moiety of the NI/pyridine or NI/pyrazole C^N ligand is *directly cyclometalated* (i.e., the C atom of the C−Pt bond is from the 3 or 5 position of the NI unit). The model complex with the 1-phenylpyrazole C^N ligand was also prepared (**Pt-1**). With the 4-pyrazole/NI ligand, two isomers with five- and six-membered chelate rings were obtained (**Pt-2** and **Pt-3**). With the 4-pyridine/NI ligand, however, only the complex with a five-membered coordination ring was obtained (**Pt-4**). With direct cyclometalation of the NI moiety, UV−vis absorption of the complexes are red-shifted from 314 nm (**Pt-1**) to 443 nm (e.g., for **Pt-3**). Compared to the complexes reported previously by us with NI groups dangling on the ppy ligand, absorption in the visible region is greatly increased with direct cyclometalation (ε increased from 4120 to 21 900 M^{-1} cm^{-1} for **Pt-3**). Complexes **Pt-2**, **Pt-3**, and **Pt-4** show RT phosphorescence (630−674 nm) in fluid solutions. The phosphorescence lifetimes of the complexes with the NI moiety directly cyclometalated (e.g., τ = 61.9 μs for **Pt-3**) are significantly longer than the model complex ppyPt(acac) (τ = 2.6 μs). We attribute the long-lived red emission of the platinum(II) complexes with the NI moiety directly cyclometalated (**Pt-2**, **Pt-3**, and **Pt-4**) to the intraligand triplet excited state (^{3}IL). This assignment is supported by the nanosecond time-resolved transient difference absorption spectra and spin-density analysis (by DFT calculations). The transient absorption spectra ($T_1 \rightarrow T_n$ transitions, $n > 1$) were rationalized by TDDFT calculations, which also support the ^{3}IL assignment of the T_1 excited states of **Pt-2**, **Pt-3**, and **Pt-4**. The light-harvesting ability and long-lived ^{3}IL excited state of the complexes (especially **Pt-3**) were employed for TTA-based upconversion. For **Pt-3**, the complex with the light-harvesting effect in the visible region and long-lived ^{3}IL excited state, the TTET is highly efficient ($K_{SV} = 3.07 \times 10^5$ M^{-1}; $k_q = 5.1 \times 10^9$ M^{-1} s^{-1}) and the upconversion quantum yield was determined as Φ_{UC} = 14.1%, whereas other complexes show negligible upconversion capabilities under the same conditions. Our strategy of accessing the long-lived emissive ^{3}IL excited state of organic fluorophore by direct cyclometalation of a chromophore will be useful for the future design of transition-metal complexes and applications as optical/electrical materials.

4. EXPERIMENTAL SECTION

4.1. Apparatus. NMR spectra were recorded on a 400 MHz Varian Unity Inova spectrophotometer. Mass spectra were recorded with Q-TOF Micro and MALDI micro MX spectrometers. UV−vis absorption spectra were recorded on a HP8453 UV−vis spectrophotometer. Fluorescence spectra were recorded on a JASCO FP-6500 or a Sanco 970 CRT spectrofluorometer. Luminescent lifetimes were measured on a Horiba Jobin Yvon Fluoro Max-4 (TCSPC) instrument.

dx.doi.org/10.1021/ic201254w | *Inorg. Chem.* 2011, 50, 11446–11460

4.2. Synthesis. *Preparation of* ***Pt-1****.* Under Ar, **L-1** (288.0 mg, 2.0 mmol) and K_2PtCl_4 (415.0 mg, 1.0 mmol) were added to a mixture of 2-ethoxyethanol (6 mL) and water (2 mL). The suspension was heated at 80 °C for 16 h. After cooling to RT, water (10 mL) was added and the precipitate was filtered, washed with water (2 × 20 mL), and dried in vacuum oven at 50 °C for 5 h. The precipitate was treated with acetylacetone (Hacac, 0.30 g, 3.0 mmol) and Na_2CO_3 (1.06 g, 10.0 mmol) in 2-ethoxyethanol (6 mL) at 100 °C for 16 h. After cooling to RT, water (10 mL) was added and the precipitate was filtered and washed with water (2 × 20 mL). The crude product was purified by column chromatography (silica gel; CH_2Cl_2/hexane, 1:1, v/v). A white solid was obtained. Yield: 51.3%, 0.22 g. ^{1}H NMR (400 MHz, $CDCl_3$): δ 7.92 (d, J = 2.8 Hz, 1H), 7.79 (d, J = 2.0 Hz, 1H), 7.56−7.54 (m, 1H), 7.13−7.07 (m, 3H), 6.51 (t, J = 2.8 Hz, 1H), 5.48 (s, 1H), 1.99 (s, 3H), 1.97 (s, 3H). ^{13}C NMR (100 MHz, $CDCl_3$): δ 185.67, 183.56, 144.41, 137.53, 131.64, 125.55, 125.02, 123.85, 122.11, 109.96, 106.17, 102.37, 27.88, 26.44. MALDI-HRMS. Calcd for $C_2H_{14}N_2O_2Pt$ ($[M]^+$): m/z 437.0703. Found: m/z 437.0735. Anal. Calcd for $C_{14}H_{14}N_2O_2Pt$ (C_6H_{14}): C, 45.88; H, 5.39; N, 5.35. Found: C, 45.92; H, 5.33; N, 5.40.

Preparation of ***L-2****.* ^{58}*N*-Butyl-4-bromonaphthalimide (664.4 mg, 2 mmol) and pyrazole (204.0 mg, 3 mmol) were dissolved under N_2 in 2 mL of acetonitrile and 2 mL of toluene, $CsCO_3$ (1.30 g, 4 mmol), EDTA·2Na (134.5 mg, 0.4 mmol), and CuI (38.1 mg, 0.2 mmol) were added, and the mixture was heated to reflux for 24 h. The crude product was purified by flash chromatography on silica gel (eluent: CH_2Cl_2). A yellow solid was obtained. Yield: 68.9%, 0.44 g. ^{1}H NMR (400 MHz, $CDCl_3$): δ 8.66 (d, J = 8.0 Hz, 2H), 8.54 (d, J = 8.4 Hz, 1H), 7.92 (d, J = 2.4 Hz, 2H), 7.82−7.77 (m, 2H), 6.64 (t, J = 4.0 Hz, 1H), 4.21 (t, J = 7.6 Hz, 2H), 1.78−1.71 (m, 2H), 1.50−1.44 (m, 2H), 0.99 (t, J = 7.6 Hz, 3H). ^{13}C NMR (100 MHz, $CDCl_3$) δ 164.18, 163.66, 142.57, 142.12, 132.02, 131.72, 131.19, 130.81, 129.52, 127.95, 127.95, 126.75, 123.09, 122.87, 122.49, 108.23, 40.59, 30.38, 20.57, 14.03. TOF MS ES. Calcd for $C_{19}H_{18}N_3O_2$ ($[M + H]^+$): m/z 320.1399. Found: m/z 320.1398.

General Procedures for the Synthesis of ***Pt-2*** *and* ***Pt-3****.* Under Ar, **L-2** (319.4 mg, 1.0 mmol) and K_2PtCl_4 (207.5 mg, 0.5 mmol) were added to a mixture of 2-ethoxyethanol (6 mL) and water (2 mL). The suspension was heated at 80 °C for 16 h. After cooling to RT, water (10 mL) was added and the precipitate was filtered, washed with water (2 × 20 mL), and dried in vacuum oven at 50 °C for 5 h. The precipitate was treated with Hacac (150.0 mg, 1.5 mmol) and Na_2CO_3 (530.0 mg, 5.0 mmol) in 2-ethoxyethanol (6 mL) at 100 °C for 20 h. After cooling to RT, water (10 mL) was added and the precipitate was filtered and washed with water (2 × 20 mL). The crude product was purified by column chromatography (silica gel, CH_2Cl_2). **Pt-2** was obtained as an orange solid. Yield: 3.2%, 10 mg. **Pt-3** was obtained as a yellow solid. Yield: 9.6%, 40 mg.

Pt-2. ^{1}H NMR (400 MHz, $CDCl_3$): δ 8.51 (s, 1H), 8.49 (d, J = 2.8 Hz, 1H), 8.42 (d, J = 6.8 Hz, 1H), 8.27 (d, J = 8.4 Hz, 1H), 7.80 (d, J = 2.4 Hz, 1H), 7.61 (t, J = 7.6 Hz, 1H), 6.65 (t, J = 2.8 Hz, 1H), 5.50 (s, 1H), 4.15 (t, J = 7.6 Hz, 2H), 2.06 (s, 3H), 2.00 (s, 3H), 1.76−1.70 (m, 2H), 1.50−1.43 (m, 2H), 0.98 (t, J = 7.2 Hz, 3H). ^{13}C NMR (100 MHz, $CDCl_3$): δ 185.69, 183.80, 164.34, 163.79, 142.96, 138.50, 135.14, 131.26, 128.37, 127.30, 126.62, 125.42, 124.66, 123.63, 118.62, 117.63, 107.28, 102.52, 40.28, 30.27, 20.49, 13.88. MALDI-HRMS. Calcd for $C_{24}H_{23}N_3O_4Pt$ ($[M]^+$): m/z 612.1336. Found: m/z 612.1286. Anal. Calcd for $C_{24}H_{23}N_3O_4Pt$: C, 47.06; H, 3.78; N, 6.86. Found: C, 47.12; H, 3.74; N, 6.81.

Pt-3. ^{1}H NMR (400 MHz, $CDCl_3$): δ 8.60 (d, J = 2.0 Hz, 1H), 8.56 (d, J = 8.4 Hz, 1H), 8.43 (d, J = 3.2 Hz, 1H), 8.38 (d, J = 8.0 Hz, 1H), 8.26 (d, J = 8.0 Hz, 1H), 7.76 (d, J = 8.0 Hz, 1H), 6.74 (t, J = 2.8 Hz, 1H), 5.55 (s, 1H), 4.18 (t, J = 7.6 Hz, 2H), 2.06 (s, 3H), 2.04 (s, 3H), 1.75−1.71 (m, 2H), 1.55−1.42 (m, 2H), 0.98 (t, J = 7.6 Hz, 3H). ^{13}C NMR (100 MHz, $CDCl_3$): δ 186.68, 185.18, 165.15, 163.84, 142.32, 139.47, 133.24, 132.01, 131.15, 129.80, 129.54, 123.86, 123.01, 118.43, 113.64, 110.05, 102.56, 40.32, 30.46, 20.62, 14.01. MALDI-HRMS. Calcd for $C_{24}H_{23}N_3O_4Pt$ ($[M]^+$): m/z 612.1336. Found: m/z 612.1370. Anal. Calcd for $C_{24}H_{23}N_3O_4Pt$ (C_6H_{14}): C, 51.57; H, 5.34; N, 6.01. Found: C, 51.61; H, 5.33; N, 5.96.

Preparation of ***Pt-3*** *by Microwave Irradiation.* In order to increase the yield and shorten the reaction time, microwave irradiation was applied to the preparation of **Pt-3**. Under Ar, **L-2** (191.6 mg, 0.6 mmol) and K_2PtCl_4 (124.5 mg, 0.3 mmol) were added to a mixture of 2-ethoxyethanol (6 mL) and water (2 mL). The suspension was irradiated by microwave (75 W) for 0.5 h. After cooling to RT, water (10 mL) was added and the precipitate was filtered, washed with water (2 × 20 mL), and dried in vacuum oven at 50 °C for 3 h. The precipitate was treated with Hacac (90.0 mg, 0.9 mmol) and Na_2CO_3 (318.0 mg, 3.0 mmol) in 2-ethoxyethanol (4 mL) by microwave (75 W) for 0.5 h. After cooling to RT, water (10 mL) was added and the precipitate was filtered and washed with water (2 × 20 mL). The crude product was purified by column chromatography (silica gel, CH_2Cl_2). **Pt-3** was obtained as a yellow solid. Yield: 50.1%, 92.0 mg. Different from the preparation with a conventional heating method, **Pt-2** was not found in the reaction mixture with microwave irradiation.

Preparation of ***L-3****.* 2-Butyl-6-bromonaphthalimide (332.0 mg, 1.00 mmol), pyridine-2-boronic acid *N*-phenyldiethanolamine ester (isopropyl alcohol; 505.0 mg, 1.25 mmol), $[Pd(PPh_3)_4]$ (58.0 mg, 0.05 mmol), 50% aqueous K_2CO_3 (3.68 g, 13.30 mmol), CuI (76.0 mg, 0.4 mmol), MeOH (1.5 mL), and toluene (7.5 mL) were mixed. The mixture was degassed with Ar and refluxed for 8 h. After cooling, the solvent was evaporated under reduced pressure and the residue was extracted with CH_2Cl_2. The organic layer was dried with Na_2SO_4 and then evaporated to dryness. The crude product was purified by column chromatography (silica gel; CH_2Cl_2/petroleum ether, 2:1, v/v). A yellow solid was obtained. Yield: 24.2%, 80.0 mg. ^{1}H NMR (400 MHz, $CDCl_3$): δ 8.85 (d, J = 4.4 Hz, 1H), 8.68 (d, J = 7.6 Hz, 1H), 8.64 (d, J = 7.2 Hz, 1H), 8.51 (d, J = 8.4 Hz, 1H), 7.94−7.87 (m, 2H), 7.75 (t, J = 7.2 Hz, 1H), 7.64 (d, J = 7.6 Hz, 1H), 7.46−7.43 (m, 1H), 4.22 (t, J = 7.6 Hz, 2H), 1.78−1.72 (m, 2H), 1.50−1.45 (m, 2H), 1.00 (t, J = 7.6 Hz, 3H). ^{13}C NMR (100 MHz, $CDCl_3$): δ 164.49, 164.24, 157.64, 150.03, 144.47, 137.15, 132.67, 131.41, 130.84, 129.90, 129.05, 128.39, 127.41, 125.36, 123.25, 123.16, 123.09, 40.54, 30.45, 20.61, 14.03. TOF MS ES. Calcd for $C_{21}H_{19}N_2O_2$ ($[M + H]^+$): m/z 331.1447. Found: m/z 331.1438.

Preparation of ***Pt-4****.* Under Ar, **L-3** (165 mg, 0.5 mmol) and K_2PtCl_4 (104.0 mg, 0.25 mmol) were added to a mixture of 2-ethoxyethanol (6 mL) and water (2 mL). The suspension was heated at 80 °C for 16 h. After cooling to RT, water (10 mL) was added and the precipitate was filtered, washed with water (2 × 20 mL), and dried in vacuum oven at 50 °C for 5 h. The precipitate was treated with Hacac (75 mg, 0.75 mmol) and Na_2CO_3 (265 mg, 2.5 mmol) in 2-ethoxyethanol (6 mL) at 100 °C for 20 h. After cooling to RT, water (10 mL) was added and the precipitate was filtered and washed with water (2 × 20 mL). The crude product was purified by column chromatography (silica gel; CH_2Cl_2/hexane, 1:1, v/v). A light-yellow solid was obtained. Yield: 71.9%, 0.11 g. ^{1}H NMR (400 MHz, $CDCl_3$): δ 9.13 (d, J = 4.8 Hz, 1H), 8.79 (s, 1H), 8.60 (d, J = 8.8 Hz, 1H), 8.45 (d, J = 6.4 Hz, 1H), 8.14 (d, J = 8.0 Hz, 1H), 7.91 (t, J = 8.0 Hz, 1H), 7.64 (t, J = 8.0 Hz, 1H), 7.21 (t, J = 6.0 Hz, 1H), 5.51 (s, 1H), 4.18 (t, J = 7.6 Hz, 2H), 2.10 (s, 3H), 2.05 (s, 3H), 1.76−1.71 (m, 2H), 1.55−1.45 (m, 2H), 0.99 (t, J = 7.2 Hz, 3H). ^{13}C NMR (100 MHz, $CDCl_3$): δ 186.24, 185.01, 167.36, 164.76, 164.37, 148.62, 144.17, 138.38, 134.12, 128.58, 128.17, 127.47, 127.13, 124.01, 123.72, 122.20, 120.91, 102.93, 40.50, 30.49, 28.32, 27.42, 20.68, 14.07. MALDI-HRMS. Calcd for $C_{26}H_{24}N_2O_2Pt$ ($[M]^+$): m/z 623.1384. Found: m/z 623.1393. Anal. Calcd for $C_{26}H_{24}N_2O_4Pt$ ($2H_2O$): C, 47.34; H, 4.28; N, 4.25. Found: C, 47.46; H, 4.20; N, 4.23.

4.3. Electrochemical Measurements. Electrochemical measurements were made using a CHI630D instrument. A conventional three-electrode configuration consisting of a glassy working electrode, a platinum wire counter electrode, and a $Ag/AgNO_3$ reference electrode was used. The solvent in all measurements was CH_2Cl_2, and the supporting electrolyte was 0.1 M $[Bu_4N]PF_6$. A scan rate of 100 mV s^{-1} was typically employed. Under these experimental conditions, the ferrocene/ferrocenium couple was determined to be +0.22 V vs $Ag/AgNO_3$.

4.4. TTA-Based Upconversion. A diode-pumped solid-state laser was used for excitation of upconversion. The samples were purged

with N_2 or Ar for 15 min before measurement. The upconversion quantum yields were determined with 4-dicyanomethylene-6-[*p*-(dimethylamino)styryl]-2-methyl-4*H*-pyran as the quantum yield standards (Φ = 0.10 in CH_2Cl_2), and the quantum yields were calculated with eq 1,[39] where Φ_{UC}, A_{unk}, I_{unk}, and η_{unk} represent the quantum yield, absorbance, integrated photoluminescence intensity, and refractive index of the solvents (eq 1). The equation is multiplied by a factor of 2 in order to give the maximum quantum yield as units.[39]

$$\Phi_{UC} = 2\Phi_{std}\left(\frac{A_{std}}{A_{unk}}\right)\left(\frac{I_{unk}}{I_{std}}\right)\left(\frac{\eta_{unk}}{\eta_{std}}\right)^2 \quad (1)$$

4.5. Nanosecond Time-Resolved Transient Difference Absorption Spectroscopy. The nanosecond time-resolved transient difference absorption spectra were recorded on a LP 920 laser flash photolysis spectrometer (Edinburgh Instruments, Livingston, U.K.). The samples were purged with N_2 or Ar for 15 min before measurement. The samples were excited with a 355 nm laser, and the transient signals were recorded on a Tektronix TDS 3012B oscilloscope.

4.6. Triplet State Quantum Yield (Φ_T). A comparative method was used for determination of the triplet state quantum yield.[38a] The triplet state quantum yields (Φ_T) of the complexes were determined with benzophenone in the actinometer (Φ_T = 1.00; the molar extinction coefficient of the triplet state at 530 nm is 7220 ± 320 M^{-1} cm^{-1}).[38b] The Φ_T values of the complexes were calculated according to eq 2.[38a,c] Absorbance of the sample and that of benzophenone at 355 nm were brought to the same (where the samples were in an excited state).

$$\Phi_T = \Phi_R \frac{\Delta OD_T \Delta\varepsilon_R}{\Delta OD_R \Delta\varepsilon_T} \quad (2)$$

In the above equation, Φ_T, ΔOD_T, and $\Delta\varepsilon_T$ represent the triplet state quantum yield, optical intensity change, and difference between the triplet and singlet molar extinction coefficients of the samples. Φ_R, ΔOD_R, and $\Delta\varepsilon_R$ are the corresponding values for the standard (benzophenone). Here an approximation was used; absorption of the triplet excited state of the complexes at the bleach is close to zero.

4.7. DFT Computational Methods. The gas-phase geometry optimizations were calculated using the B3LYP functional with the 6-31G(d) basis set (for platinum, the LanL2DZ basis set was used) as implemented.[59] The vertical excitation energy was calculated with the TDDFT method based on the singlet ground-state geometry. The spin density of the triplet state was calculated from the energy-minimized geometries of the triplet states. The nanosecond transient absorption of our cyclometalated platinum(II) complexes was treated as UV−vis absorption of the T_1 state of the complexes. The vertical excitation energies (transitions of $T_1 \rightarrow T_2$, $T_1 \rightarrow T_3$, etc.) were calculated with the TDDFT method. Calculations are with dichloromethane as the solvent (polarized continuum model, PCM).[60] Please note that the bleaching effect was not included in the calculated transient absorption spectra. All calculations were performed using *Gaussian 09W* software (Gaussian, Inc.).[61]

■ ASSOCIATED CONTENT

Ⓢ Supporting Information

Compound characterization data and emission spectra (^1H and ^{13}C NMR and HRMS). This material is available free of charge via the Internet at http://pubs.acs.org.

■ AUTHOR INFORMATION

Corresponding Author

*E-mail: zhaojzh@dlut.edu.cn. Group homepage: http://finechem.dlut.edu.cn/photochem

■ ACKNOWLEDGMENTS

We thank the NSFC (20972024 and 21073028), Fundamental Research Funds for the Central Universities (DUT10ZD212 and DUT11LK19), the Royal Society (UK) and NSFC (China−UK Cost-Share program, 21011130154), Ministry of Education (SRFDP-200801410004 and NCET-08-0077), State Key Laboratory of Chemo/Biosensing and Chemometrics (2008009), and Dalian University of Technology for financial support.

■ REFERENCES

(1) Williams, J. A. G. *Top. Curr. Chem.* **2007**, *281*, 205−268.
(2) Wong, W. Y.; Ho, C. L. *Coord. Chem. Rev.* **2009**, *253*, 1709−1758.
(3) Yin, B.; Niemeyer, F.; Williams, J. A. G.; Jiang, J.; Boucekkine, A.; Toupet, L.; Le Bozec, H.; Guerchais, V. *Inorg. Chem.* **2006**, *45*, 8584−8596.
(4) (a) Lakowicz, J. R. *Principles of Fluorescence Spectroscopy*, 2nd ed.; Kluwer Academic/Plenum Publishers: New York, 1999. (b) Valeur, B. *Molecular Fluorescence: Principles and Applications*; Wiley-VCH Verlag GmbH: New York, 2001.
(5) Ma, B.; Djurovich, P. I.; Thompson, M. E. *Coord. Chem. Rev.* **2005**, *249*, 1501−1510.
(6) Wu, W.; Cheng, C.; Wu, W.; Guo, H.; Ji, S.; Song, P.; Han, K.; Zhao, J.; Zhang, X.; Wu, Y.; Du, G. *Eur. J. Inorg. Chem.* **2010**, 4683−4696.
(7) Wu, W.; Wu, W.; Ji, S.; Guo, H.; Zhao, J. *Eur. J. Inorg. Chem.* **2010**, 4473−4482.
(8) Wu, W.; Wu, W.; Ji, S.; Guo, H.; Song, P.; Han, K.; Chi, L.; Shao, J.; Zhao, J. *J. Mater. Chem.* **2010**, *20*, 9775−9786.
(9) Wu, W.; Wu, W.; Ji, S.; Guo, H.; Zhao, J. *Dalton Trans.* **2011**, *40*, 5953−5963.
(10) Ji, S.; Wu, W.; Wu, W.; Guo, H.; Zhao, J. *Angew. Chem., Int. Ed.* **2011**, *50*, 1626−1629.
(11) Zhao, Q.; Li, F.; Huang, C. *Chem. Soc. Rev.* **2010**, *39*, 3007−3030.
(12) Goldsmith, J. I.; Hudson, W. R.; Lowry, M. S.; Anderson, T. H.; Bernhard, S. *J. Am. Chem. Soc.* **2005**, *127*, 7502−7510.
(13) Zhang, J.; Du, P.; Schneider, J.; Jarosz, P.; Eisenberg, R. *J. Am. Chem. Soc.* **2007**, *129*, 7726−7727.
(14) Condie, A. G.; González-Gómez, J. C.; Stephenson, C. R. J. *J. Am. Chem. Soc.* **2010**, *132*, 1464−1465.
(15) Zhang, R.; Yu, X.; Ye, Z.; Wang, G.; Zhang, W.; Yuan, J. *Inorg. Chem.* **2010**, *49*, 7898−7903.
(16) Xiong, L.; Zhao, Q.; Chen, H.; Wu, Y.; Dong, Z.; Zhou, Z.; Li, F. *Inorg. Chem.* **2010**, *49*, 6402−6408.
(17) Ji, S.; Guo, H.; Yuan, X.; Li, X.; Ding, H.; Gao, P.; Zhao, C.; Wu, W.; Wu, W.; Zhao, J. *Org. Lett.* **2010**, *12*, 2876−2879.
(18) Ji, S.; Wu, W.; Wu, W.; Song, P.; Han, K.; Wang, Z.; Liu, S.; Guo, H.; Zhao, J. *J. Mater. Chem.* **2010**, *20*, 1953−1963.
(19) Guo, H.; Ji, S.; Wu, W.; Wu, W.; Shao, J.; Zhao, J. *Analyst* **2010**, *135*, 2832−2840.
(20) Guo, H.; Muro-Small, M. L.; Ji, S.; Zhao, J.; Castellano, F. N. *Inorg. Chem.* **2010**, *49*, 6802−6804.
(21) Zhou, G. J.; Wang, Q.; Wong, W. Y.; Ma, D.; Wang, X. L.; Lin, Z. Y. *J. Mater. Chem.* **2009**, *19*, 1872−1883.
(22) He, Z.; Wong, W.; Yu, X.; Kwok, H.; Lin, Z. *Inorg. Chem.* **2006**, *45*, 10922−10937.
(23) Brooks, J.; Babayan, Y.; Lamansky, S.; Djurovich, P. I.; Tsyba, I.; Bau, R.; Thompson, M. E. *Inorg. Chem.* **2002**, *41*, 3055−3066.
(24) Borisov, S. M.; Klimant, I. *Anal. Chem.* **2007**, *79*, 7501−7509.
(25) Hanson, K.; Tamayo, A.; Diev, V. V.; Whited, M. T.; Djurovich, P. I.; Thompson, M. E. *Inorg. Chem.* **2010**, *49*, 6077−6084.
(26) Huang, J.; Xu, Y.; Qian, X. *Org. Biomol. Chem.* **2009**, *7*, 1299−1303.
(27) Zhou, Y.; Xiao, Y.; Chi, Sh.; Qian, X. *Org. Lett.* **2008**, *10*, 633−636.

(28) Tyson, D. S.; Luman, C. R.; Zhou, X.; Castellano, F. N. *Inorg. Chem.* **2001**, *40*, 4063−4071.
(29) Ryan, G. J.; Quinn, S.; Gunnlaugsson, T. *Inorg. Chem.* **2008**, *47*, 401−403.
(30) Pomestchenko, I. E.; Castellano, F. N. *J. Phys. Chem. A* **2004**, *108*, 3485−3492.
(31) Pomestchenko, I. E.; Luman, C. R.; Hissler, M.; Ziessel, R.; Castellano, F. N. *Inorg. Chem.* **2003**, *42*, 1394−1396.
(32) Sun, H.; Guo, H.; Wu, W.; Liu, X.; Zhao, J. *Dalton Trans.* **2011**, *40*, 7834−7841.
(33) Harriman, A.; Hissler, M.; Khatyr, A.; Ziessel, R. *Chem. Commun.* **1999**, 735−736.
(34) Tyson, D. S.; Castellano, F. N. *J. Phys. Chem. A* **1999**, *103*, 10955−10960.
(35) Kozlov, D. V.; Tyson, D. S.; Goze, C.; Ziessel, R.; Castellano, F. N. *Inorg. Chem.* **2004**, *43*, 6083−6092.
(36) Galletta, M.; Campagna, S.; Quesada, M.; Ulrich, G.; Ziessel, R. *Chem. Commun.* **2005**, 4222−4224.
(37) Sazanovich, I. V.; Alamiry, M. A. H.; Best, J.; Bennett, R. D.; Bouganov, O. V.; Davies, E. S.; Grivin, V. P.; Meijer, A. J. H. M.; Plyusnin, V. F.; Ronayne, K. L.; Shelton, A. H.; Tikhomirov, S. A.; Towrie, M.; Weinstein, J. A. *Inorg. Chem.* **2008**, *47*, 10432−10445.
(38) (a) Yang, H.; Zhang, Z.; Han, Z.; Yao, S. *Dyes Pigm.* **2000**, *46*, 139−143. (b) Bonneau, R.; Carmichael, I.; Hug, G. *Pure Appl. Chem.* **1991**, *63*, 289−299. (c) Reddi, E.; Jori, G.; Rodgers, M. A. J.; Spikes, J. D. *Photochem. Photobiol.* **1983**, *38*, 639−645. (d) Ji, S.; Wu, W.; Wu, Y.; Zhao, T.; Zhou, F.; Yang, Y.; Zhang, X.; Liang, X.; Wu, W.; Chi, L.; Wang, Z.; Zhao, J. *Analyst* **2009**, *134*, 958−965.
(39) Singh-Rachford, T. N.; Castellano, F. N. *Coord. Chem. Rev.* **2010**, *254*, 2560−2573.
(40) Islangulov, R. R.; Lott, J.; Weder, C.; Castellano, F. N. *J. Am. Chem. Soc.* **2007**, *129*, 12652−12653.
(41) Baluschev, S.; Yakutkin, V.; Miteva, T.; Avlasevich, Y.; Chernov, S.; Aleshchenkov, S.; Nelles, G.; Cheprakov, A.; Yasuda, A.; Müllen, K.; Wegner, G. *Angew. Chem., Int. Ed.* **2007**, *46*, 7693−7696.
(42) Chen, H.; Hung, C.; Wang, K.; Chen, H.; Fann, W. S.; Chien, F.; Chen, P.; Chow, T. J.; Hsu, C.; Sun, S. *Chem. Commun.* **2009**, 4064−4066.
(43) Keivanidis, P. E.; Baluschev, S.; Miteva, T.; Nelles, G.; Scherf, U.; Yasuda, A.; Wegner, G. *Adv. Mater.* **2003**, *15*, 2095−2098.
(44) Cheng, Y. Y.; Fückel, B.; Khoury, T.; Clady, R. G. C. R.; Tayebjee, M. J. Y.; Ekins-Daukes, N. J.; Crossley, M. J.; Schmidt, T. W. *J. Phys. Chem. Lett.* **2010**, *1*, 1795−1799.
(45) Tanaka, K.; Inafuku, K.; Chujo, Y. *Chem. Commun.* **2010**, *46*, 4378−4380.
(46) Zhao, W.; Castellano, F. N. *Inorg. Chem.* **2006**, *110*, 11440−11445.
(47) Du, P.; Eisenberg, R. *Chem. Sci.* **2010**, *1*, 502−506.
(48) Kim, H. M.; Cho, B. R. *Acc. Chem. Res.* **2009**, *42*, 863−872.
(49) Lim, C. S.; Kang, D. W.; Tian, Y. S.; Han, J. H.; Hwang, H. L.; Cho, B. R. *Chem. Commun.* **2010**, *46*, 2388−2390.
(50) Islangulov, R. R.; Kozlov, D. V.; Castellano, F. N. *Chem. Commun.* **2005**, 3776−3778.
(51) Monguzzi, A.; Mezyk, J.; Scotognella, F.; Tubino, R.; Meinardi, F. *Phys. Rev. B* **2008**, *78*, 195112−1−195112−5.
(52) Monguzzi, A.; Tubino, R.; Meinardi., F. *Phys. Rev. B* **2008**, *77*, 155122−1−155122−4.
(53) Merkel, P. B.; Dinnocenzo, J. P. *J. Lumin.* **2009**, *129*, 303−306.
(54) Baluschev, S.; Yakutkin, V.; Wegner, G.; Minch, B.; Miteva, T.; Nelles, G.; Yasuda, A. *J. Appl. Phys.* **2007**, *101*, 023101-1−023101-4.
(55) Cheng, Y. Y.; Khoury, T.; Clady, R. G. C. R.; Tayebjee, M. J. Y.; Ekins-Daukes, N. J.; Crossley, M. J.; Schmidt, T. W. *Phys. Chem. Chem. Phys.* **2010**, *12*, 66−71.
(56) (a) Zhao, J.; Ji, S.; Guo, H. *RSC Adv.* **2011**, *1*, 937−950. (b) Liu, Y.; Wu, W.; Zhao, J.; Zhang, X.; Guo, H. *Dalton Trans.* **2011**, *40*, 9085−9089.
(57) (a) Sun, J.; Wu, W.; Guo, H.; Zhao, J. *Eur. J. Inorg. Chem.* **2011**, 3165−3173. (b) Ji, S.; Guo, H.; Wu, W.; Wu, W.; Zhao, J. *Angew. Chem., Int. Ed.* **2011**, *50*, 8283−8286. (c) Wu, W.; Guo, H.; Wu, W.; Ji, S.; Zhao, J. *J. Org. Chem.* **2011**, *76*, 7056−7064. (d) Huang, L.; Zeng, L.; Guo, H.; Wu, W.; Wu, W.; Ji, S.; Zhao, J. *Eur. J. Inorg. Chem.* **2011**, 4527−4533 . (e) Wu, W.; Sun, J.; Ji, S.; Wu, W.; Zhao, J. Guo, H. *Dalton Trans.* **2011**, *40*, 11550−11561.
(58) Cristau, H.; Cellier, P. P.; Spindler, J.; Taillefer, M. *Eur. J. Org. Chem.* **2004**, 695−709.
(59) (a) Becke, A. D. *J. Chem. Phys.* **1993**, *98*, 5648−5652. (b) Ditchfild, R.; Hehre, W. J.; Pople, J. A. *J. Chem. Phys.* **1971**, *54*, 724−728.
(60) (a) Mineva, T.; Russo, N. *Int. J. Quantum Chem.* **1997**, *61*, 665−671. (b) Houjou, H.; Inoue, Y.; Sakurai, M. *J. Am. Chem. Soc.* **1998**, *120*, 4459−4470.
(61) Frisch, M. J.; Trucks, G. W.; Schlegel, H. B.; Scuseria, G. E.; Robb, M. A.; Cheeseman, J. R.; Scalmani, G.; Barone, V.; Mennucci, B.; Petersson, G. A.; Nakatsuji, H.; Caricato, M.; Li, X.; Hratchian, H. P.; Izmaylov, A. F.; Bloino, J.; Zheng, G.; Sonnenberg, J. L.; Hada, M.; Ehara, M.; Toyota, K.; Fukuda, R.; Hasegawa, J.; Ishida, M.; Nakajima, T.; Honda, Y.; Kitao, O.; Nakai, H.; Vreven, T.; Montgomery, J. A., Jr.; Peralta, J. E.; Ogliaro, F.; Bearpark, M.; Heyd, J. J.; Brothers, E.; Kudin, K. N.; Staroverov, V. N.; Kobayashi, R.; Normand, J.; Raghavachari, K.; Rendell, A.; Burant, J. C.; Iyengar, S. S.; Tomasi, J.; Cossi, M.; Rega, N.; Millam, N. J.; Klene, M.; Knox, J. E.; Cross, J. B.; Bakken, V.; Adamo, C.; Jaramillo, J.; Gomperts, R.; Stratmann, R. E.; Yazyev, O.; Austin, A. J.; Cammi, R.; Pomelli, C.; Ochterski, J. W.; Martin, R. L.; Morokuma, K.; Zakrzewski, V. G.; Voth, G. A.; Salvador, P.; Dannenberg, J. J.; Dapprich, S.; Daniels, A. D.; Farkas, Ö.; Foresman, J. B.; Ortiz, J. V.; Cioslowski, J.; Fox, D. J. *Gaussian 09*, revision A.1; Gaussian Inc.: Wallingford, CT, 2009.